Soft Matter

REVIEW

View Article Online
View Journal

Cite this: DOI: 10.1039/d1sm00621e

Evaluation of dielectric elastomers to develop materials suitable for actuation

Philippe Banet, *[a] Nouh Zeggai,[a] Jonathan Chavanne, [b] Giao T. M. Nguyen, [a] Linda Chikh,[a] Cédric Plesse,[a] Morgan Almanza, [c] Thomas Martinez, [b] Yoan Civet, [b] Yves Perriard [b] and Odile Fichet[a]

Electroactive polymers based on dielectric elastomers are stretchable and compressible capacitors that can act as transducers between electrical and mechanical energies. Depending on the targeted application, soft actuators, sensors or mechanical-energy harvesters can be developed. Compared with conventional technologies, they present a promising combination of properties such as being soft, silent, light and miniaturizable. Most of the research on dielectric elastomer actuators has focused on obtaining the highest strain, either from technological solutions using commercially available materials or through the development of new materials. It is commonly accepted that a high electrical breakdown field, a low Young's modulus and a high dielectric constant are targets. However, the interdependency of these properties makes the evaluation and comparison of these materials complex. In addition, dielectric elastomers can suffer from electromechanical instability, which amplifies their complexity. The scope of this review is to tackle these difficulties. Thus, first, two physical parameters are introduced, one related to the energy converted by the dielectric elastomer and another to its electromechanical stability. These numbers are then used to compare dielectric elastomers according to a general and rational methodology considering their physicochemical and electromechanical properties. Based on this methodology, different families of commercially available dielectric elastomers are first analyzed. Then, different polymer modification methods are presented, and the resulting modified elastomers are screened. Finally, we conclude on the trends enabling the choice of the most suitable modification procedure to obtain the desired elastomer. From this review work, we would like to contribute to affording a quick identification method, including a graphic representation, to evaluate and develop the dielectric materials that are suitable for a desired actuator.

Received 27th April 2021,
Accepted 10th November 2021

DOI: 10.1039/d1sm00621e

rsc.li/soft-matter-journal

Introduction

Electroactive polymers (EAPs) are currently receiving special attention because they offer new possibilities of application in various fields (automotive, aeronautic, computer science, electronic, *etc.*). These polymers, whose size or shape changes when they are electrically stimulated, can therefore transform electrical energy into mechanical work (actuator function), or *vice versa* (sensor function).[1–3] Compared with conventional technologies, they have the advantages of being light, silent, miniaturizable, flexible and even stretchable. Their mode of operation as well as their flexible or stretchable character, regularly gives them the name of "artificial muscles".[2,4]

Electroactive polymers can be classified into two categories according to their actuation principle: ionic EAPs and electronic EAPs.[5] The actuation mode of ionic EAPs is based on the diffusion of ions that is induced electrochemically through the material (for example, gels, conductive polymers, and ionic polymer–metal composites). Unlike ionic EAPs, electronic EAPs are insulators and include piezoelectric, ferromagnetic, and dielectric elastomers. Each type of electroactive polymer has advantages and disadvantages, making some more suitable for certain applications than others. Among them, dielectric elastomers (DEs) are actuated mainly by the Coulomb electrostatic pressure induced by the application of a high electric field between the electrodes.[6]

The actuation mechanism of dielectric elastomer actuators (DEAs) was demonstrated more than one hundred years ago by Röntgen.[7] However, it was not until the 2000s that DEAs attracted much greater attention when Pelrine *et al.* demonstrated a 100% actuation strain of a prestretched acrylic elastomer.[8] Since then, several groups have then focused on

[a] *CY Cergy Paris Université, LPPI, F-95000 Cergy, France. E-mail: philippe.banet@cyu.fr*
[b] *École Polytechnique Fédérale de Lausanne (EPFL) - Institut de Microtechnique (IMT) - Laboratoire d'Actionneurs Intégrés (LAI) - Center for Artificial Muscles (CAM), Rue de la Maladière 71B, Neuchâtel, Switzerland*
[c] *École normale supérieure Paris-Saclay, Laboratoire SATIE, France*

different aspects of DEAs, from modelling, mechanics, and materials development to applications. Lu *et al.* reviewed the theory and mechanics of dielectric elastomers.[7] Boundary value problems have been analyzed with examples on the verification of theoretical predictions *via* experiments. These problems point out the importance of electromechanical instability, which can, in several cases, be overcome by appropriate prestretching. The performances and the configurations of reported DE transducers have been summarized too, and a run through of the last developments in DE materials has been presented. Several valuable reviews have also been published recently on the development of dielectric elastomers. They deal either with all dielectric elastomer families,[6] or with specific elastomers such as silicone[9–12] or acrylics.[13] They have focused on three properties of DEs that impact the actuation, namely the Young's modulus (Y), the dielectric permittivity (ε_r), and the breakdown field (E_b), and on the methodologies used to modify these properties and tune the actuation. Due to the inter-dependency of these properties, in some of these reviews, a figure of merit that reveals the actuation-strain improvement has been introduced to facilitate the comparison of DEs.[9,10] Although the impact of modifying the properties of DEs on their electromechanical instability is discussed in these reviews, a combined appreciation of the actuation-strain improvement and electromechanical stability of DEs is lacking.

This review aims to identify the best dielectric elastomers for an intended actuator application taking into account both the energy converted by a DE and its electromechanical stability. In the first part, the actuation principle of DEs will be described. Then two physical parameters based on the three properties of DEs that impact the actuation mentioned previously (Y, ε_r and E_b) will be introduced to evaluate the actuation properties. These parameters will be used in new methodology that will be proposed for comparing and classifying the different polymer materials according to their actuation efficiency. An additional striking input of this work is the graphical presentation of each material in relation to its two physical parameters, which allows the materials or be compared quickly and their weaknesses and strengths identified. Later, these new criteria will be used to compare the different families of commercially available DEs and the different methods that have been explored to modify their properties. Finally, trends on actuation related to the modification process will be drawn. This work could quickly allow the identification of a dielectric material that is suitable for a desired actuator.

1. Principle and evaluation criterion of dielectric elastomers

In dielectric elastomer (DE) technology, an electrical potential difference is applied between the two compliant electrodes that sandwich an elastomer. Charges on the surface cause the generation of a Maxwell stress that in turn compresses the soft material and expands it laterally (Fig. 1). This process thus converts electrical energy into mechanical work.[1,2] Dielectric

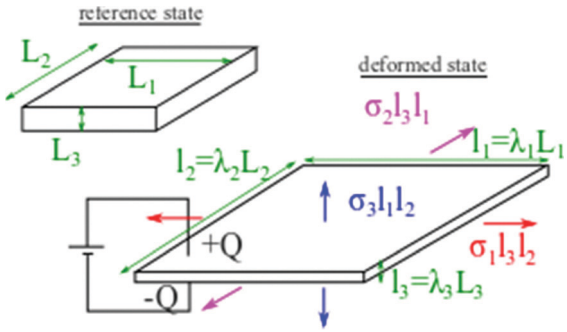

Fig. 1 Principle of actuation of a dielectric elastomer (DE) in the reference state and in the state deformed by an applied electric field.

elastomers are characterized by a fast electromechanical response, a high actuating force, a high mechanical energy density and the ability to maintain induced movement at a constant voltage. The deformation rates of this type of material are significant when the electric field is close to the breakdown field, E_b (the maximum value of the electric field that the elastomer can withstand before the occurrence of a short circuit). Depending on their composition and operating range, elastomers can show complex types of behavior, such as non-linearity, anisotropic stress softening (anisotropy induced by the Mullins effect), viscoelasticity (the Payne effect) and deviation from incompressibility.[14,15] Moreover, a strong stretch dependence of the breakdown field and of the dielectric permittivity can complexify further the electromechanical behavior of these materials.

Further to the work of Pelrine *et al.*, prestretching appears to increase the breakdown field significantly and to stabilize the electromechanical instability, which is recognized as an important mode of failure.[8] However, the use of rigid or bulky frames mitigates the high energy density of a dielectric elastomer-based actuator.

To investigate a material suitable for a dielectric actuator when prestretching is not required, we propose the introduction of two physical parameters, where one is related to the energy converted by the DEA and the other is related to its electromechanical stability, and where both of them are related to the Young's modulus (Y), the dielectric permittivity (ε_r), and the electrical breakdown field (E_b).

Suo *et al.*[16] established the relationship[1] between the deformation and the electric field E for an incompressible, isotropic and ideal dielectric elastomer (no electrostriction),

$$\sigma_i - \sigma_3 = \lambda_i \frac{\partial W_s(\lambda_1, \lambda_2, 1/(\lambda_1\lambda_2))}{\partial \lambda_i} - \varepsilon_0 \varepsilon_r E^2 \qquad (1)$$

where σ_i is the true stress with $i \in \{1;2\}$, ε_0 is the vacuum permittivity (F m^{-1}), ε_r is the relative permittivity of the material (without units), E the applied electric field (V m^{-1}), $W_s(\lambda_1,\lambda_2, 1/\lambda_1,\lambda_2)$ is the Helmholtz free energy associated with the stretching of the elastomer, σ_k is the true external stress (the force normalized by the area of the deformed state) and λ_k is the stretch along the axis k (without units) ($k \in \{1;2;3\}$).

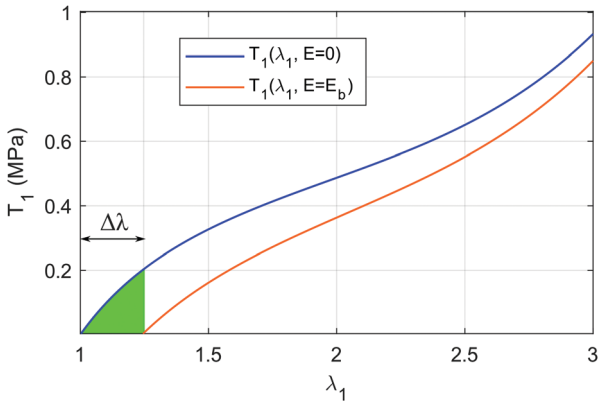

Fig. 2 Nominal stress function of the stretch at zero (blue) and the breakdown field (red) The green area corresponds to the cycle targeted.

To achieve actuation, membranes can operate in numerous ways from simple pure shear, uniaxial and biaxial plane configurations to more complex geometries such as tube and gripper.[7] Here, the pure shear configuration ($\lambda_2 = 0$) is used for comparison. Thus, work $T_1 d\lambda_1 L_1$ is only exchanged on axis 1, with

$$T_1(\lambda_1, E) = \frac{\partial W_s(\lambda_1, \lambda_2, 1/(\lambda_1\lambda_2))}{\partial \lambda_1} - \frac{\varepsilon_0 \varepsilon_r E^2}{\lambda_1}, \quad (2)$$

where $T_1(\lambda_1,E)$ is the nominal stress.

Elastomers are generally described according to a hyperelastic model, such as the Yeoh or Gent models.[17–19] Fig. 2 shows the use of a hyperelastic model to describe Elastosil 2030 from Wacker. The electromechanical cycle for energy conversion is in-between the curve at zero and the breakdown field. The green area in Fig. 2 is a relevant cycle for application which does not require pre-stretching. Its energy density (defining a figure of merit) is

$$F_{om} = \int_1^{1+\Delta\lambda} T_1(\lambda_1, 0) d\lambda_1 = W_s(\Delta\lambda) \quad (3)$$

with $\Delta\lambda + 1$ the stretch at zero nominal stress and at the breakdown field, such as $T_1(\Delta\lambda + 1, E_b) = 0$. To be able to determine the criterion of comparison, the nominal stress–stretch relationship used to estimate the energy of a cycle is considered as being linear (Fig. 2) $\frac{\partial W_s}{\partial \lambda_1} = Y(\lambda_1 - 1)$, where Y is Young's modulus. The stretch, $\Delta\lambda$, is $\frac{\varepsilon_0 \varepsilon_r E_b^2}{Y}$ and the energy F_{om} becomes $\varepsilon_0 \varepsilon_r E_b^2$.

To maximize the energy $F_{om} = \varepsilon_0 \varepsilon_r E_b^2$ of a dielectric elastomer, we have to increase the electric field, which is limited by the breakdown field (E_b), and increase the material's relative permittivity (ε_r) on the one hand and on the other hand maximize the strain, $\frac{\varepsilon_0 \varepsilon_r E_b^2}{Y}$, for which we need to decrease the material's Young's modulus (Y), as has been studied by Della Schiava *et al.*[20]

However, this approach is not self-sufficient due to the electromechanical instability, as defined by Zhao *et al.*,[21] and often leads to premature breakdown. The stability of the actuator must therefore also be considered. Indeed, the objective is to obtain an actuator which guarantees safe and permanent working conditions until electrical breakdown by avoiding electromechanical instability. A criterion of stability until electrical breakdown has been previously developed by Suo *et al.*[16] and Chavanne *et al.*[22] and is given by:

$$\frac{\delta\sigma_1}{\delta\lambda_1} - \frac{1}{\lambda_1}\left(\sigma_1 + \varepsilon_0 \varepsilon_r E_b^2\right) > 0 \quad (4)$$

where λ_1 is the stretch of the actuator in the deformed direction. Considering a linear stress–strain characteristic (Fig. 2), eqn (4) becomes

$$R = \frac{Y}{\varepsilon_0 \varepsilon_r E_b^2} > 1, \quad (5)$$

an expression related to one over the strain. Here, we deduce two important statements. First, to ensure an electromechanically stable actuator the stretch is necessarily limited to 2 (*i.e.*, 100% strain). Second, the Young's modulus, so as to follow the energy density, must increase to keep R higher than 1.

In summary, increasing $F_{om} = \varepsilon_0 \varepsilon_r E_b^2$ while targeting a small ratio $R = \frac{Y}{\varepsilon_0 \varepsilon_r E_b^2}$ allows the energy density of any dielectric polymer and its capability to have a large deformation to be enhanced. However, to guarantee a stable behavior until the electrical breakdown and to avoid electromechanical instability, the ratio R should be kept higher than 1. Hence, the figure of merit, $F_{om} = \varepsilon_0 \varepsilon_r E_b^2$, and the ratio, $R = \frac{Y}{\varepsilon_0 \varepsilon_r E_b^2}$, are well suited to analyze the compromise that should be found between the electric field, the relative permittivity and the Young's modulus.

As a result, to compare the performances of different materials and the effects of their modification, this review is based on collecting the breakdown voltages, relative permittivities and Young's moduli of different available elastomers from which F_{om} and R are calculated. In addition, a target area is defined where materials should present both a high energy density and stable behavior regarding the electromechanical instability. This target area is limited by R values higher than 1.2 to add a margin for reasons previously explained. R values that are woo high will lead to materials that are too rigid to have interesting actuation properties, and a maximal value of 2 for R is therefore set; hence, R should be between 1.2 and 2. The F_{om} limits are based on work densities between 0.1 and 0.5 J cm^{-3} that are generally required for dielectric actuators[23] and even up to 1 J cm^{-3} for work energies.[24] It is therefore desirable to reach these values today.

Various families of commercial elastomers, especially polyacrylates,[8,25] silicones,[25,26] polyurethanes,[27] rubbers,[28,29] and copolymers,[30] are then reviewed to evaluate their performance as dielectric elastomer actuators.[27,31] Specifically, their different characteristics (relative permittivity, breakdown field and Young's modulus) are reported in Table 1. It is noteworthy that, while the dielectric permittivity values vary only slightly for a given material according to different authors, the reported values of the Young's modulus and breakdown fields can be strongly dependent on the

Table 1 Dielectric and mechanical properties of different families of elastomers

Polymer	Abbreviation on figures	ε_r	E_b (V μm^{-1})	Y (MPa)	F_{om} (J cm^{-3})	$R = Y/F_{om}$	Ref.
Polyacrylates							
VHB 3 M 4910	VHB	4.7	17–31	0.4–2.3	0.01–0.04	10.0–191	27 and 32
Polyurethanes							
TPU-LPT4210-UT50	TPU-LPT4210	6[a]	218	3.36[b]	2.53	1.33	27
Bayfol (EA102)	Bayfol	7.1[a]	130	1.44[b]	1.06	1.36	27
Deerfield PT6100S	PU Deerfield	7[c]	160	17	1.59	10.7	29
Estane TPU5888	Estane	6	50	0.01	0.13	0.08	33
Silicones							
Elastosil LR3005/50	LR3005/50	2.9[e]	115	0.28	0.35	0.82	34
Elastosil 2030/50	LR2030/50	2.8	100	0.4	0.25	1.6	35
Elastosil p7670	p7670	3.1	30	0.28	0.02	11.3	36
Elastosil LR3043/50[d]	LR3043/50	2.8[e]	144[f]	0.53	0.51	1.0	34
Elastosil LR3043/30[d]	LR3043/30	2.8[e]	123	0.25	0.38	0.67	34
Elastosil RT625[d]	RT625	2.8[e]	50	0.3	0.06	4.84	34
Silastic LC50 2004	LC50 2004	3	105	0.33	0.29	1.13	37
Silastic 3481	Sil3481	3.64	50	0.61	0.08	7.50	38
Sylgard 186	Sylg 186	2.8[c]	144	0.7	0.51	1.36	29
Sylgard 184[d]	Sylg 184	2.39[g]	27	2.2	0.02	142.5	39
Dow Corning[h]	HS3	2.8[c]	72	0.125	0.13	0.97	29
Nusil CF19-2186	CF19	2.8[c]	235	1	1.37	0.73	29
BlueStar MF620U	MF620U	3.13	55.9	0.37	0.09	4.27	40
Pow XLR 630[4]	XLR630	2.9[e]	134	0.244	0.46	0.53	34
Fluorosilicone[h] Dow Corning 730	DC730	6.9[c]	80	0.5	0.39	1.28	29
Other families							
Fluoroelastomer L143HC	L143HC	12.7[c]	32	2.5	0.12	21.7	29
HNBR[i]	HNBR	12.5[c]	50	1.6	0.28	5.78	28
SBS[j]	SBS	3.9	65	0.5	0.14	3.42	41
Natural rubber latex	Polyisoprene	2.7[c]	67	0.85	0.11	7.92	29
SEBS[k]	SEBS	3	45	0.16[42]	0.05	3.0	43 and 44
EPDM[l]	EPDM	3	20	0.09	0.01	8.47	31

[a] At 1/8 Hz. [b] Module at 50% strain. [c] At 1 kHz. [d] The commercial formula contains SiO_2 as an additive. [e] At 0.1 Hz. [f] 23 V μm^{-1} in the data sheet. [g] At 1 Hz. [h] Centrifuged to remove fillers from commercial formula. [i] Hydrogenated nitrile butadiene rubber (commercial elastomer). [j] Styrene–butadiene–styrene elastomer (commercial elastomer). [k] Styrene–ethylene–butadiene–styrene elastomer (commercial elastomer). [l] Ethylene–propylene–diene monomer rubber (commercial elastomer).

measurement setups and thus vary greatly from one study to another.[27,32] Both parameters F_{om} and $R = Y/F_{om}$ were systematically calculated from the noted characteristics, allowing positioning of the materials on R–F_{om} graphs. The measurement frequency of ε_r is specified when it is known and most of the materials are not prestretched before analysis, or prestretching is not specified in the cited studies.

2. Native commercial dielectric elastomers

Among polar elastomers, polyacrylates, and in particular VHB 4910 (as marketed by 3M) (Fig. 3), have the advantage of being provided in the form of a film and of having high elongation at break values (>600%, allowing significant actuation).[27] They

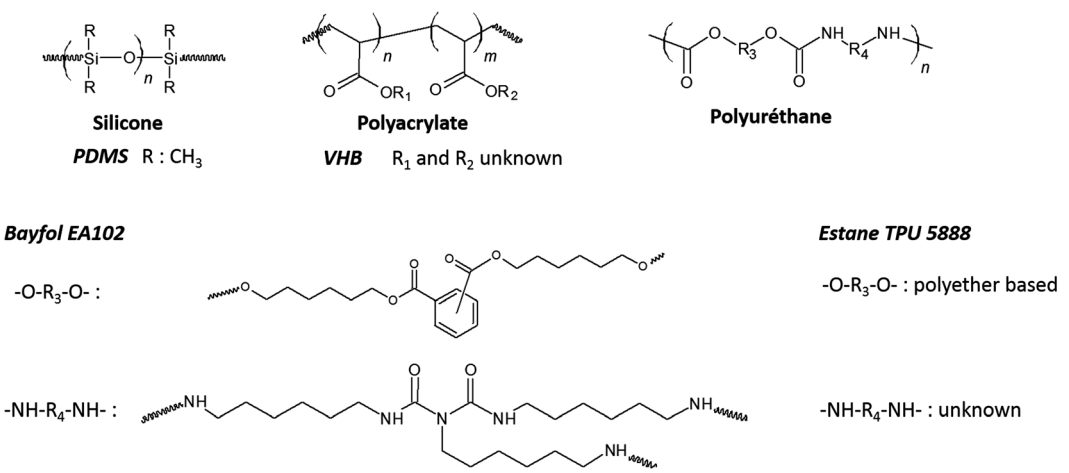

Fig. 3 Generalized polymer backbone structures of common dielectric elastomers.

show a dielectric permittivity of about 4.7 and a breakdown field E_b in the range of 17–31 V μm^{-1} (Table 1). Hence, they exhibit low values for the figure of merit (F_{om} < 0.04 J cm^{-3}). Their reported elasticity moduli vary greatly (from 0.4 to 2.3 MPa), which place them in an R–F_{om} plot in an area that is far away from the targeted area defined with the criteria presented in the first part of this review (the solid grey-shaded part in Fig. 4). In addition, these materials are viscoelastic, resulting in long response times, with a delay of several hundred milliseconds to obtain a stable state after the application of stress, and hysteresis during cycling. Another point is the dependence of the leakage current on the humidity and temperature, which renders the material sensitive to these parameters. Consequently, the number of cycles before failure decreases when the relative humidity increases, and the actuation performance also decreases when the temperature increases.[27]

Considering the polyurethane family (PUs), the presence of polar urethane groups gives these materials a higher permittivity (>6) compared with polyacrylates (Fig. 3 and Table 1). They also have a higher breakdown field, which varies from 50 V μm^{-1} for Estane TPU5888 to 218 V μm^{-1} for PU(TPU-LPT4210-UT50). Except for Estane TPU5888, they present high values of the figure of merit F_{om} (>1 J cm^{-3}). Moreover, their Young's moduli vary greatly from 1.44 to 17 MPa according to the proportion of urethane groups, as well as the nature of the segments (R_3 and R_4) linked to these groups, which can be either rigid or flexible (Fig. 3). Thus some formulations such, as Bayfol EA102 (synthesized by the polyaddition of a polyhexamethylenediisocyanate (Desmodur N100) and a non-commercial polyester polyol based on hexanediol and phthalic anhydride (P200H/DS)) or TPU-LPT4210-UT50 (a thermoplastic elastomer obtained from a non-identified formulation and presenting a high level of creep),[27] combine a high F_{om} value and an R ratio in the target area defined for dielectric elastomer actuator applications (Fig. 4). However, PUs generally show a low electrical resistance and are sensitive to moisture uptake, which leads to a reduction in their actuation performance during operation.[27]

A last class of polar elastomers is fluoroelastomers (most often copolymers of poly(vinylidene fluoride) with trifluoroethylene, tetrafluoroethylene or hexafluoropropylene). They show interesting thermal and chemical stabilities, and they have the highest dielectric permittivities (ε_r > 12) due to the presence of polar bonds. However, they have the drawback of having concomitantly moderate breakdown fields and high Young's moduli (>2 MPa), which tend to limit their deformation rates during actuation.[29] Fig. 4 outlines an example of a fluoroelastomer (L143HC) showing a high R value and a low figure of merit.

In contrast to polar elastomers, slightly polar elastomers (polyisoprene, HNBR, SEBS, SBS or EPDM) suffer from a low dielectric permittivity, and a moderate breakdown field as well as a low Young's modulus, leading to high R values and low figures of merit (Fig. 4).

Among non-polar elastomers, silicones are the family with the most commercially available products. Despite their low permittivity values ($\varepsilon_r \approx 2.8$) compared with the other families already mentioned, they remain good candidates because they can withstand high electrical fields (up to 235 V μm^{-1} for Nusil CF19 2186), which allow values of F_{om} of at least 10 times higher than the VHB elastomer. Moreover, due to their typically low Young's moduli (between 0.125 and 1 MPa), some of them show an R ratio close to the target area. For instance, Nusil CF19 2186, a silicone based on polydimethylsiloxane (PDMS) obtained by hydrosilylation reaction, combines a high F_{om} value and an R ratio close to the target area (Fig. 5). In addition, silicone elastomers present numerous advantages: fast response times (a few ms to a few tens of ms) with low or no hysteresis during cycling; performance stability over a wide temperature range; and low moisture absorption.[27] It is noteworthy that, among silicone elastomers, fluorosilicones such as

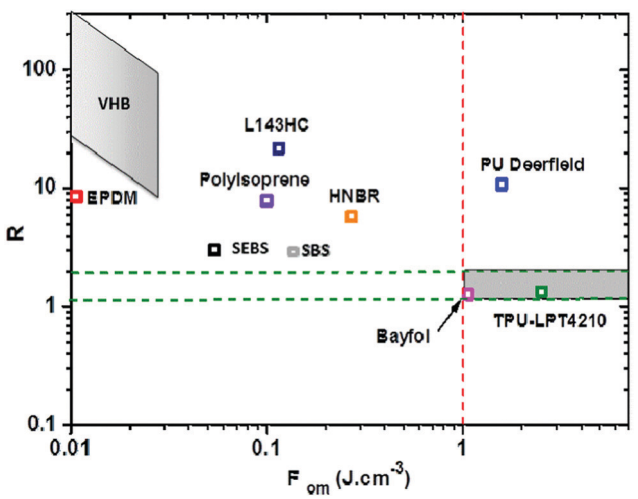

Fig. 4 Comparison between the F_{om} and R parameters of different dielectric elastomers: polyacrylate (VHB), polyurethane and other families.

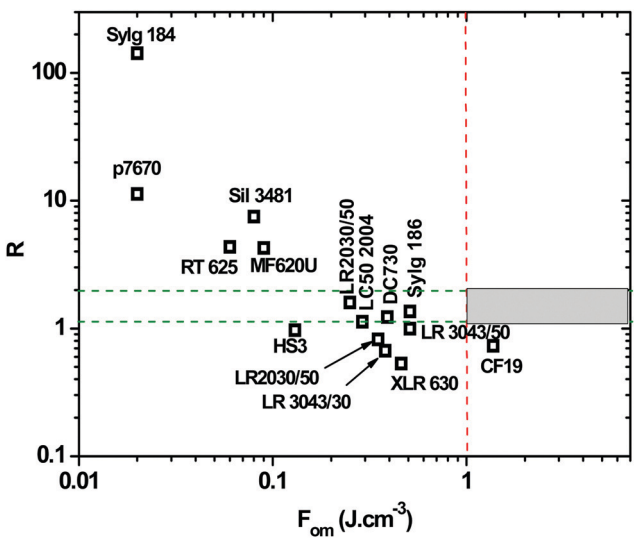

Fig. 5 Comparison between the F_{om} and R parameters of silicone materials.

DC730 are a class of dielectric elastomers that have a high relative permittivity ($\varepsilon_r \approx 6.9$) due to the highly polar C–F bond, which makes up for a lower electrical field to reach the target figure of merit value.

From this first analysis, it appears that few commercially available products have the electromechanical characteristics required to make a performant dielectric actuator stable over time when used in their native form.

3. Improvement of dielectric elastomer properties

To enhance the actuation performance of dielectric elastomers, different modification methods have been reported. Thus, DE electrical and mechanical properties can be improved either by engineering the design and/or processing the devices, or by modifying the elastomer. The elastomer modification could be extrinsic if the elastomer is blended with other polymers and/or fillers, or intrinsic if it is chemically modified. These different pathways and their effects are now presented.

3.1 Electrochemical property improvement *via* engineering

Prestretching is an efficient way to modify the breakdown strength of elastomers and to improve their actuation performance, in particular the actuated strain (Table 2).

The effect of prestretching on the elastomer actuation performance was first published by Pelrine *et al.*,[8] demonstrating that the breakdown strengths of polyacrylate films and silicones can be enhanced thanks to this mechanical constraint.[8,25,45] For instance, the breakdown strength of VHB 4910 increased from 17–31 to 412 V μm^{-1} after a biaxial (300%,300%) prestrain, and from 17–31 to 239 V μm^{-1} when a uniaxial (540%,75%) prestrain was applied[25,45] (Table 2). This improvement was confirmed in another study using a biaxial (300%,300%) prestrain leading to an increase in the breakdown strength to 205 V μm^{-1}.[25] This phenomenon has also been observed for prestretched Nusil CF19-2186 (biaxial prestrain 45%,45%) and Dow Corning HS3 (uniaxial prestrain 280%,0%) silicones, whose breakdown strengths increased from 235 to 350 V μm^{-1}, and from 72 to 128 V μm^{-1}, respectively. However, the mechanism responsible for this improvement is not yet fully understood, and the studies have mainly been focused on dielectric permittivity evolution during prestretching. Kofod *et al.*[25] have shown that permittivity of VHB 4910 is modified slightly (ε_r = 4.7 to ε_r = 4.5) after biaxial prestretching (400%,400%), while other studies have described a decrease in ε_r, from 4.7 to 3.7[47] or 2.6,[48] after the same prestretch. This decrease, observed when the polymer is stretched, may be due to dipoles losing their freedom of alignment.

Other studies have demonstrated that prestretching does not affect the elastomer modulus in directions different from the direction of stretching[49] and that prestretching allows the suppression of the pull-in instability inside the VHB network.[50–52] Nevertheless, there exists an optimum prestretching ratio for each type of elastomer and each prestretch mode. For example, Akbari *et al.*[53] have demonstrated that a biaxial prestretch of 150% is sufficient for suppression of the pull-in instability in a PDMS elastomer, and that a higher prestretch leads to a stiffening of the elastomer and an increase in the actuation voltage.

Finally, it should be noted that Young's moduli are rarely given for the prestretched materials and are considered to be only slightly changed after prestretching.[49]

Therefore, it is now accepted that an improvement in the actuation properties using prestretching is assigned to both the suppression of pull-in instability and the increase in breakdown strength.

A large increase in the breakdown field is thus obtained upon prestretching, while the relative permittivity is moderately affected. This improves the value of the figure of merit F_{om} and, as a result, improves the actuation strain. Simultaneously, considering that the Young's moduli are kept constant the

Table 2 Properties of prestretched commercial dielectric elastomers. Non-prestretched elastomers are also specified for comparison (values in bold type)

Elastomer	Abbreviation on figures	Prestrain (x%,y%)	ε_r	E_b (V μm^{-1})	Y (MPa)	F_{om} (J cm^{-3})	Y/F_{om}	Ref.
Polyacrylates								
VHB 3M 4910	VHB	**(0,0)**	**4.7**[a]	**17–31**	**0.4–2.3**	**0.01–0.04**	**10–191**	**27 and 32**
	VHB(15,15)	(15,15)	4.8[a,d]	55	3[f,d]	0.13	23.3	8 and 45
	VHB(300,300)	(300,300)	4.8[a,d]	412	3[f,d]	7.22	0.42	8 and 45
	VHB(540,75)	(540,75)	4.8[a,d]	239	3[f,d]	2.43	1.24	8 and 45
	VHB(200,200)	(200,200)	5.0[b]	76	0.8[g]	0.26	3.13	46
	—	(300,300)	4.5[c]	205	N.S.	N.S.	N.S.	25
Silicones								
Nusil CF19-2186	CF19	**(0,0)**	**2.8**[a]	**235**	**1**	**1.37**	**0.73**	**29**
	CF19(15,15)	(15,15)	2.8[a,d]	160	1[f,d]	0.64	1.58	8 and 45
	CF19(45,45)	(45,45)	2.8[a,d]	350	1[f,d]	3.04	0.33	8 and 45
	CF19(100,0)	(100,0)	2.8[a,d]	181	1[f,d]	0.81	1.23	8 and 45
Dow Corning[e] (HS3)	HS3	**(0,0)**	**2.8**[a]	**72**	**0.125**	**0.13**	**0.97**	**29**
	HS3(14,14)	(14,14)	2.8[a,d]	72	0.1[f,d]	0.13	0.78	8 and 45
	HS3(68,68)	(68,68)	2.8[a,d]	110	0.1[f,d]	0.30	0.33	8 and 45
	HS3(280,0)	(280,0)	2.8[a,d]	128	0.1[f,d]	0.41	0.25	8 and 45

N.S.: not specified. [a] At 1 kHz. [b] At 1 Hz. [c] At 0.1 Hz. [d] Value before prestretching. [e] Centrifuged to remove fillers from the commercial formula. [f] Effective module. [g] At 10% strain.

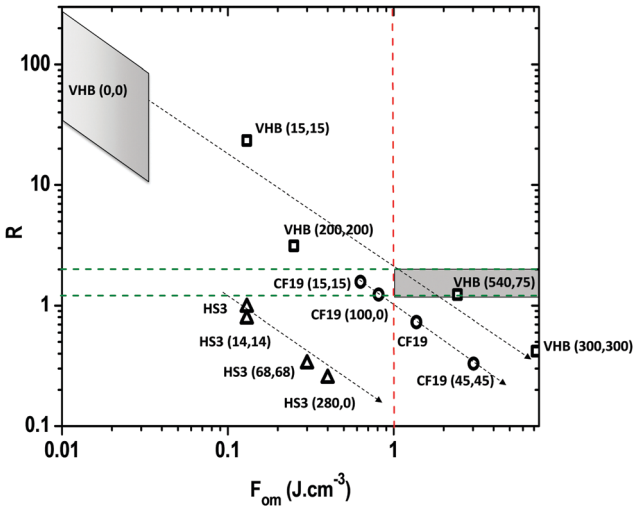

Fig. 6 Effect of pre-stretching on the F_{om} and R parameters of polyacrylates (VHB 3M 4910 (□), Nusil CF19-2186 (○) and Dow Corning HS3 (Δ)).

value of the R ratio decreases. Thus, as summarized in Fig. 6, where the R ratio is represented as a function of F_{om}, pre-stretching VHB and silicone elastomers allows them to be shifted along a line with a minus slope, making them come close to or reach the target area. For instance, uniaxially prestretched VHB 4910 (540%,75%) is very close to the target area, unlike VHB 4910 which has not been prestretched. The same result is obtained for Nusil CF19-2186 when this material is prestretched: its actuation performance is improved and to be close to the target area. Furthermore, it is noteworthy on this plot that when the Young's modulus of a dielectric elastomer is smaller than 1.2 MPa (such as HS3 silicone) the target area cannot be reached with this material, whatever its energy density.

3.2 Extrinsic modifications

Another way to modify the electromechanical properties of dielectric elastomers is to combine them with other polymers, fillers or plasticizers, and these different paths are now described.

3.2.1 Polymer association. A performing dielectric elastomer can be achieved by associating a dielectric polymer with a polar polymer (or copolymer). They can be combined without any reaction between the two polymers by blending or by creating an interpenetrating polymer network architecture (Fig. 7).

The addition of a polar polymer to a low-dielectric-constant polymer allows its dielectric permittivity to be increased, as has been done to improve the intrinsic low relative permittivity of PDMS. Table 3 hereafter summarizes the characteristics of the initial elastomer (denoted in bold type) and those of materials based on blends.

The embedding of low percentages (<6 wt%) of undoped poly(3-hexylthiophene) (PHT), a soluble conjugated polymer with a strong polarization, in a commercial PDMS (TC-5005) increases its dielectric permittivity from ε_r = 4.6 to 13.8 (6 wt% PHT). Simultaneously, a slight increase from 0.5 to 3 of the dielectric loss (ε''), was observed at low frequencies indicating an increase in dissipative loss, which explains the breakdown voltage decrease from E_b = 14 to 8.5 V μm^{-1}.[54] In addition, an unexpected reduction was observed in the elasticity modulus from 100 to 46 kPa, which was assigned to a decrease in the PDMS matrix crosslinking density in the presence of PHT. These variations are reflected by a moderated value of the figure of merit for these polymer blends (lower than 0.01 J cm^{-3}) and a decrease of the R ratio from 12.5 to 6.1–5.2, which remains high. The same authors have also shown that it is possible to obtain similar effects by blending a two-component PU (Poly74–Polytek) with the same PDMS. The obtained material with 40 vol% PU is characterized by a dielectric constant ($\varepsilon_r \approx 15.3$ at 10 Hz) that is higher than those of the single PDMS ($\varepsilon_r \approx 4.6$) and PU ($\varepsilon_r \approx 7.5$), while the elasticity modulus remains unchanged (Y = 0.1 MPa).[55] As observed for blending with PHT, this material is also characterized by a high value of dielectric loss ($\varepsilon'' > 3$) at low frequencies (<300 Hz). The authors reported that, regardless of the electric field applied, the polymer blend with PU has higher actuation deformations

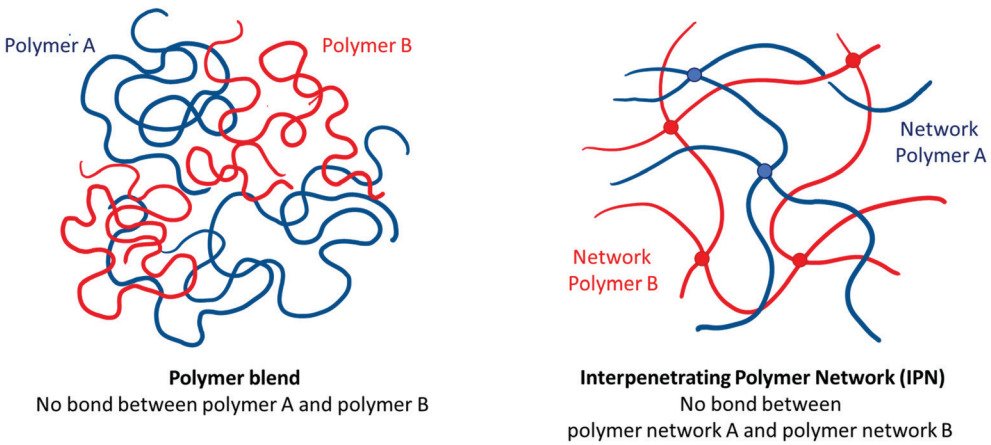

Fig. 7 Schematic of a polymer blend (left) and an interpenetrating polymer network (right) architecture.

Table 3 Properties of silicones blended with different polymers

Polymers	Abbreviation on figures	ε_r	E_b (V μm^{-1})	Y (MPa)	F_{om} (J cm^{-3})	$R = Y/F_{om}$	Ref.
TC-5005 A/B-C[a]	**TC**	**4.6**[b]	**14**	**0.10**[d]	**0.008**	**12.5**	**54**
+PHT (1 wt%)	TC + PHT_1 wt%	5.6[b]	8.1	0.02[d]	0.003	6.1	54
+PHT (6 wt%)	TC + PHT_6 wt%	13.8[b]	8.5	0.046[d]	0.009	5.2	54
+PU (40 vol%)	TC + PU_40 vol%	15.3[b]	5.6	0.1	0.004	23.5	55
PDMS MJK4/13	**MJK**	**3.5**[c]	**93**	**0.25**	**0.27**	**0.9**	**56**
+PDMS-*co*-PEG (5 wt%)	MJK + PDMS-*co*-PEG 5 wt%	4.4[c]	103	0.12	0.41	0.3	56

[a] Bicomponent PDMS containing fillers (A/B), with component C as the additive. [b] At 10 Hz. [c] At 0.1 Hz. [d] At 100% stretching.

than the starting PDMS, but a weaker breakdown field (E_b = 5.6 V μm^{-1}) due to a detected interfacial polarization. Thus, even with PU-based blends allowing a higher actuation deformation, these PDMS-based materials also maintain a low figure of merit.

Polyethylene glycol (PEG), another type of polar polymer, can also be associated with silicone to increase the latter's dielectric permittivity. To avoid demixing, PDMS$_n$-*co*-PEG multiblock-copolymers were used as compatibilizers. These multiblock-copolymers were synthesized with various PEG proportions by varying the number of dimethylsiloxane units in the PDMS blocks (n) from 81 to 3.[56] Despite their high dielectric permittivity of up to 21 at 1 Hz, these copolymers, with a high dielectric loss, are too conductive to be used as elastomers for a dielectric actuator. By contrast, when a 5 wt% copolymer containing 38 vol% PEG is blended in the commercial silicone matrix (Wacker, MJK4/13), dispersed nodules are formed and the PDMS dielectric permittivity increases from ε_r = 3.5 to ε_r = 4.4 (at 0.1 Hz).[56] Simultaneously, the dielectric loss increase is contained ($\tan\delta < 0.01$), the elastic modulus is reduced from 0.25 to 0.12 MPa, and the breakdown field is increased from 93 ± 7 to 103 ± 4 V μm^{-1}. Thus, the F_{om} and R parameters vary from 0.27 J cm^{-3} and 0.9 for the pure PDMS to 0.41 J cm^{-3} and 0.3 for the blend. This modification therefore seems useful for increasing the figure of merit of elastomers and bringing them close to the target area. However, the R ratio is divided by 3.

These studies show that blends of silicones with polar polymers (polyhexylthiophene, polyurethane, polyethylene glycol, *etc.*) can significantly increase the silicone dielectric permittivity, and synergies can even be observed at times. However, the elasticity modulus decreases simultaneously, while the breakdown field can be slightly improved in some blends.

The association of crosslinked polymers (polymer networks) is an efficient method to obtain polymer blends that are stable over time (with an absence of demixing or evolution of the morphology over time). This type of architecture, called an interpenetrating polymer network (IPN), has already been explored with success for the development of dielectric actuators, and Table 4 summarizes the characteristics of such an architecture.

The VHB electrical breakdown resistance is improved when it is included inside an IPN architecture, as shown with VHB–TMPTMA IPNs.[57] More specifically, polyacrylate networks (VHB 4905 and VHB 4910) have been associated with trimethylolpropanetrimethacrylate (TMPTMA) networks in an IPN architecture (Fig. 8). For this, a VHB film is bi-axially stretched to 400% and swollen with TMPTMA which is then crosslinked. VHB 4905 and VHB 4910 films containing 6.6 wt% and 5.2 wt% TMPTMA networks, respectively, retain a prestretch of 275 and 244%, respectively. This association therefore allows the VHB network to remain prestretched without the application of any external force. These VHB–TMPTMA IPNs were characterized by weaker dielectric constants but higher Young's moduli, and higher breakdown fields than those of the VHB starting networks. In addition, IPNs are less viscoelastic than VHB networks. These results show that the interpenetration of an acrylate network within a VHB network improves the actuation performance and can bring VHB near to the target area (Fig. 11).

Table 4 Properties of different elastomers based on the interpenetrating polymer network architecture. The text in bold type correspond to the single networks

Polymers	Abbreviations on figures	ε_r	E_b (V μm^{-1})	Y (MPa)	F_{om} (J cm^{-3})	$R = Y/F_{om}$	Ref.
VHB 3M 4910	**VHB**	**4.7**[f]	**17–31**	**0.4–2.3**	**0.01–0.04**	**10.0–191**	**27 and 32**
VHB 3M 4910	**VHB(300,300)**	**4.8**[f,b]	**412**	**3**[a,b]	**7.22**	**0.42**	**8 and 45**
VHB 3M 4910–TMPTMA IPN	IPN VHB–TMPTMA (244,244)	3.2[g]	418	4.15[d]	4.95	0.84	57
VHB 3M 4905–TMPTMA IPN	IPN VHB–TMPTMA (275,275)	2.4[g]	265	3.94[d]	1.49	2.64	57
Elastosil LR3043/30[c]	**LR3043/30**	**2.9**[h]	**130**	**0.253**	**0.43**	**0.58**	58
LR3043/30–BS12 IPN 70–30 wt%	IPN LR3043/30	13[h]	45	0.255	0.23	1.09	
PDMS^y (M = 23 × 10^4 g mol^{-1})	**PDMS^y**	**3.1**[i]	**92**	**0.1**[e]	**0.23**	**0.43**	46
PDMS^y–PUUS IPN 95–5 wt%	IPN PDMS^y–PUUS_5	4[i]	63	0.1[e]	0.14	0.71	
PDMS^y–PUUS IPN 90–10 wt%	IPN PDMS^y–PUUS_10	4.5[i]	44	0.2[e]	0.08	2.59	
PDMS^x (M = 7 × 10^4 g mol^{-1})	**PDMS^x**	**2.9**[i]	**124**	**0.2**[e]	**0.4**	**0.51**	46
PDMS^x–PUUS IPN 80–20 wt%	IPN PDMS^x–PUUS_20	10.6[i]	11	0.6[e]	0.01	141	

[a] Effective modulus. [b] Value before prestretching. [c] The commercial formula contains SiO_2. [d] Biaxial Young's modulus. [e] At 10% strain. [f] At 1 kHz. [g] At 10 Hz. [h] At 0.1 Hz. [i] At 1 Hz.

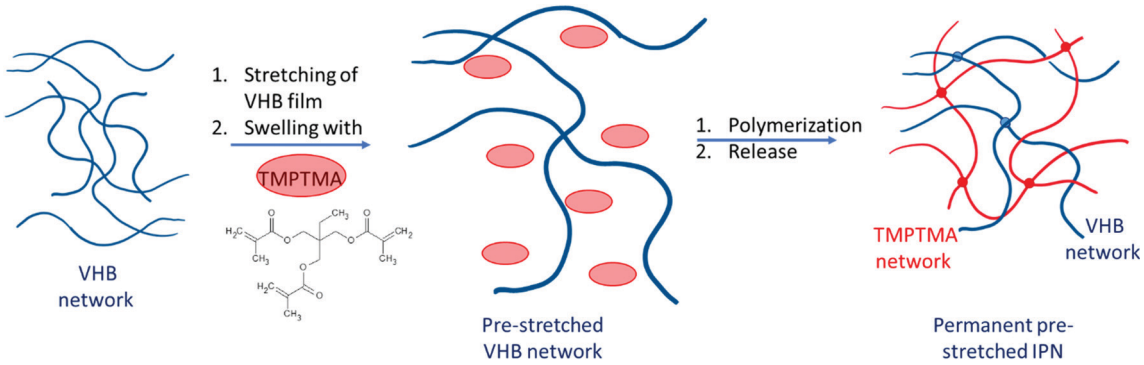

Fig. 8 VHB–TMPTMA IPN synthesis.

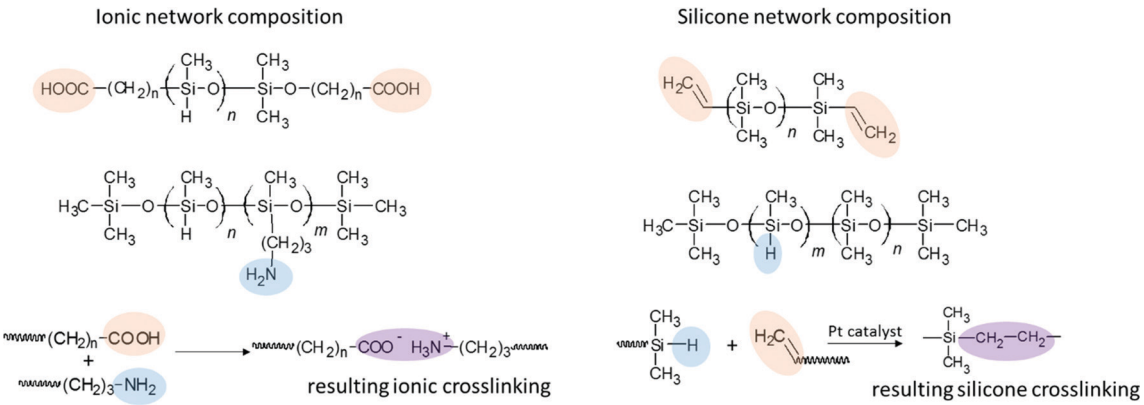

Fig. 9 Chemical structures of ionic and silicone IPNs.

Silicone–silicone-based IPNs have also been developed[58] (Fig. 9). Commercial silicones (Elastosil LR3043, Elastosil RT625 or Powersil XLR630) crosslinked *via* hydrosilylation are combined with another silicone network, crosslinked by ionic interaction. This latter network is synthesized from carboxyl-terminated PDMS (BS-12 or BS-15), and PDMS with pendant aminopropyl groups (AMS-162). On the one hand, the permittivity (at 0.1 Hz) is increased from $\varepsilon_r \approx 2.9$ for the single Elastosil LR3043 network to $\varepsilon_r \approx 13$ for the LR3043/BS-12 (70/30) IPN, while the breakdown voltage decreases (E_b = 130 V μm^{-1} for the LR3043 network and E_b = 45 V μm^{-1} for the IPN). Finally, even though it has self-healing properties, this IPN shows a figure of merit F_{om} = 0.23 J cm^{-3} and an R value of 1.09. Thus, the introduction of an ionic network in a silicone network allows the dielectric permittivity to be increased but reduces the F_{om} value due to the reduction in breakdown voltage.

IPNs based on poly(urethane-urea-siloxane) and PDMS have also been developed to provide better dielectric elastomer actuators.[46] For this, a poly(urethane-urea-siloxane) bearing pendant carboxylic acid functions (PUUS) was synthesized and then mixed in different proportions (5, 10 and 20 wt%) with PDMS network precursors of different molar weights ((7, 23 and 37) × 10^4 g mol^{-1}). A small amount of polydimethylsiloxane grafted with polyethylene glycol chains (PDMS-*g*-PEO) was added to the mixture to promote the PDMS/PUUS compatibility. Finally, tetraethyl orthosilicate (TEOS) was added as a crosslinking agent, allowing the PDMS network formation while PUUS was physically crosslinked by hydrogen bonds (Fig. 10). The higher the polyurethane proportion, the higher the Young's modulus of the IPN. The greatest increase is obtained for the PDMS network with the highest crosslinking density (*i.e.*, the precursor with the lowest molar weight) containing 20 wt% PUUS (the largest amount of the polar network) (Y = 0.2 MPa and 0.6 MPa for the reference PDMS and IPN, respectively). Association of the PUUS and PDMS networks in an IPN architecture leads to an increase in the dielectric permittivity compared with that of the reference PDMS network. Thus, a maximum dielectric permittivity (10.6 at 1 Hz) is obtained for the PDMS (7 × 10^4 g mol^{-1})/PUUS (80/20) IPN. In addition, the electric breakdown field value collapses from E_b = 124 to 11 V μm^{-1} when the proportion of PUUS is increased. This decrease is explained as being due to the surface porosity of the materials created during network formation, which increases with the urethane proportion. Finally, the electromechanical properties of these materials were characterized by measuring the deformation under an applied electric field. The higher the molar weight of PDMS, the greater the deformation. The maximum elongation (7.1%) was measured on the IPN PDMS^y–PUUS_10 for a 20 V μm^{-1} field while it did not have the highest permittivity. This observation can be

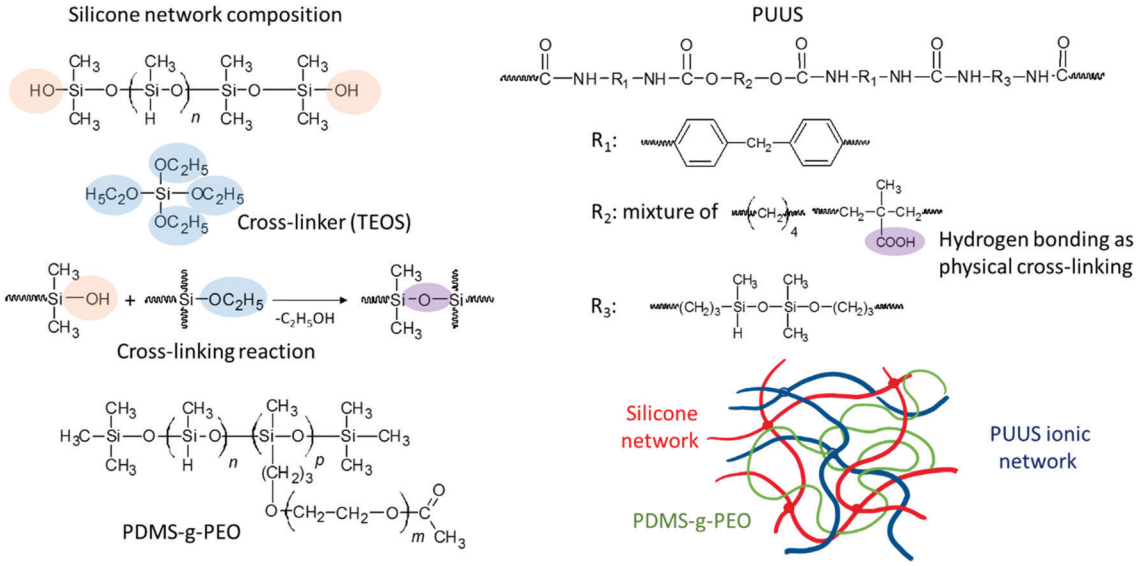

Fig. 10 PUUS/PDMS IPN chemical structures and scheme.

explained by its lower modulus. It can be seen on the R–F_{om} plot that the IPN PDMS^{y}–PUUS_10 is closer to the target area than IPN PDMS^{x}–PUUS_20, which confirms the relevance of this graph (Fig. 11). The figure of merit of these IPNs is lower than that of the PDMS network. Indeed, for a PDMS^{y} (23×10^4 g mol^{-1}) network, it decreases from 0.23 J cm^{-3} to 0.14 and 0.08 J cm^{-3} when it is combined with 5 and 10 wt% PUUS, respectively. This tendency thus leads to an opposite effect to that observed with VHB-based IPNs, which is the consequence of the large decrease in the electrical breakdown of the PDMS/PUUS IPN.

In summary, these results show that associating polymers in an interpenetrating polymer network architecture is an efficient method for increasing the material's dielectric constant. This behavior is in line with the results described on polymer blends. However, the effects on the Young's modulus and the breakdown field are different according to the examples encountered. The Young's modulus increases in the VHB–TMPTMA and PDMS–PUUS IPNs while it remains unchanged for the LR3043–BS12 IPNs. The electrical breakdown field is strongly affected by the nature of the polar partner. In a VHB–TMPTMA IPN, combining a neutral polar partner network, the breakdown field varies slightly in comparison with a pre-stretched starting network. Otherwise, for a partner network containing ionic functions (carboxylic acid or ionic crosslinks), the breakdown field decreases more markedly as, for example, in LR3043–BS12 compared with the PDMS–PUUS IPNs. However, this architecture remains of interest for improving the actuation properties of dielectric elastomers.

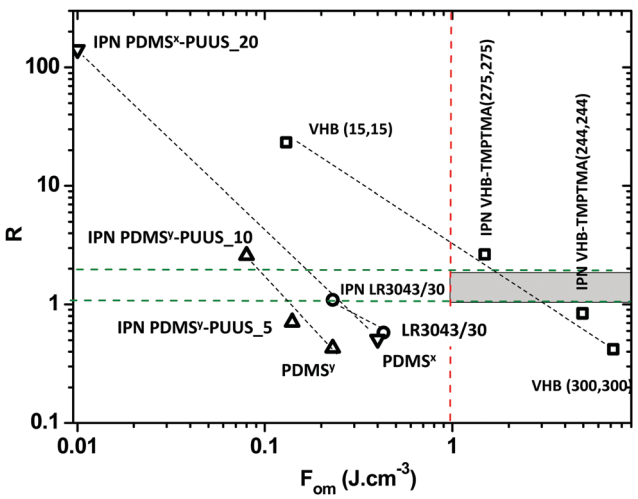

Fig. 11 Comparison between the F_{om} and R parameters of interpenetrating polymer networks based on VHB (squares) and silicones (triangles and circles).

3.2.2 Composites. The permittivity of elastomers can also be improved by incorporating high-permittivity (nano)particles,[9] such as ceramics, $BaTiO_3$,[59–61] TiO_2,[38,62,63] or $CaCu_3Ti_4O_{12}$,[40,64] whose relative permittivity is greater than $\varepsilon_r = 1000$ or electrically conductive particles such as carbon black (CB),[43] graphene,[65–67] carbon nanotubes[66,68,69] or conducting polymers.[70] The effects of adding electrically conductive fillers will be described first and then those of non-conductive fillers.

3.2.2.1 Electrically conductive fillers. When adding conductive fillers, it is essential not to exceed the percolation threshold (P_c), *i.e.*, to stay in a state where the particles are separated from each other to keep the insulating properties of the matrix. Thus, only low contents of conductive fillers are encountered. In addition, the nature, size and shape of the fillers, the dispersion or interfacial state between the matrix and fillers, *etc.*,[71] must also be taken into account but will not be dealt with in detail in this work. Results are presented in Table 5, and Fig. 12 allows the positioning of these materials in relation to the target area and shows the effects of adding conductive fillers.

Table 5 Properties of different elastomers modified by adding conductive fillers. Values in bold type correspond to the unfilled materials

Matrix (name in the figure)	Filler	Amount	ε_r	E_b (V μm^{-1})	Y (MPa)	F_{om} (J cm^{-3})	$R = Y/F_{om}$	Ref.
SEBS	**0**	**0**	**3**	**45**	**0.16**[42]	**0.054**	**3.0**	43
	CB	0.5 vol%	3	18	N.S.	0.009	—	
	CB	3.5 vol%	11	4	N.S.	0.002	—	
v-PDMS[d] (v-PDMS)	**0**	**0**	**3.3**[a]	**37**	**0.20**	**0.04**	**5.0**	68
	PDMS-MWCNT	0.05 wt%	3.56[a]	27	0.22	0.02	9.6	
Silastic 3481 (Sil3481)	**0**	**0**	**3.1**[b]	**45**	**0.52**	**0.056**	**9.3**	65
	TGNP	1.6 wt%	18.3[b]	36	1.2	0.21	5.7	
OH-PDMS (OH-PDMS)	**0**	**0**	**2.3**[c]	**66**	**0.48**[e]	**0.09**	**5.4**	70
	PANI in PDVB shell	15 vol%	3.3[c]	51	0.28[e]	0.08	3.7	

N.S.: not specified. [a] At 100 kHz. [b] At 1 kHz. [c] At 100 Hz. [d] Vinyl telechelic PDMS, M_n = 159 000 g mol^{-1}. [e] At 50% strain.

Many studies have shown that adding conductive fillers is a highly effective method to increase the elastomer permittivity, but this is coupled with a drop in the breakdown voltage. For instance, adding more than 1.0 vol% carbon black (CB) to a poly(styrene–ethylene–butadiene–styrene) (SEBS) matrix ($\varepsilon_r \approx 3$) increases the relative permittivity of the composite material while maintaining low dielectric losses as long as the percolation threshold is not reached (P_c = 4.62 vol% CB).[43] However, the breakdown field is divided by 3 (from E_b = 45 V μm^{-1} to E_b = 18 V μm^{-1}) as soon as 0.5 vol% CB is added, and by 11 (E_b = 4 V μm^{-1}) with 3.5 vol% CB. Hence, the increase in the dielectric constant (from $\varepsilon_r \approx 3$ to $\varepsilon_r \approx 11$) is not enough to compensate for the breakdown field downfall and to improve the elastomer properties for DEA applications. However, in some cases, the actuation performance of dielectric elastomers has been improved by using conductive fillers with a non-conductive shell. Thus, an actuation twice as high as that of the reference silicone matrix was obtained at 27 V μm^{-1} when multiwall carbon nanotubes (MWCNTs) functionalized covalently with PDMS (10–20 nm diameter) were included in a silicone matrix.[68] According to the authors, this functionalization allows a homogeneous dispersion of PDMS-*g*-MWCNTs in the silicone matrix and a decrease in the interfacial defects between the particles and the polymer matrix, which strongly reduces the breakdown voltage and increases the dielectric losses. When the variations of the material characteristics are examined separately, adding a small amount (0.05 wt%) of PDMS-*g*-MWCNT fillers slightly increases the permittivity at 100 kHz from $\varepsilon_r \approx 3.3$ for PDMS to $\varepsilon_r \approx 3.56$ while the Young's modulus remains almost the same (from 0.20 MPa to 0.22 MPa). Thus, the figure of merit F_{om} = 0.02 J cm^{-3} is decreased and R = 9.7 is increased. Hence, despite the authors reporting an increase in actuation at a given voltage, as the breakdown field decreases from E_b = 37 to E_b = 27 V μm^{-1}, the maximum achievable actuation remains almost unchanged. As a consequence, the addition of this conductive filler moves the material away from the target area (Fig. 12).

Conversely, the actuation performance of a Silastic 3481 silicone-based DEA is improved by the addition of thermally expanded graphene nanoplates (TGNPs) and the composite is placed closer to the target area (Fig. 12).[65] Indeed, for contents lower than 1.6 wt% TGNP filler, the volume resistivity of composites is greater than 10^{13} Ω cm and close to that of the initial silicone matrix (10^{14} Ω cm). Consequently, a low dielectric loss at 1 kHz is maintained (<0.2). Simultaneously, ε_r increases from 3.1 for the reference silicone to 18.3 for a composite material containing 1.6 wt% TGNP. In addition, the Young's modulus is doubled while the breakdown field decreases slightly from 45 V μm^{-1} to 36 V μm^{-1}. Hence, the addition of TGNP fillers allows the figure of merit of Silastic 3481 to almost quadruple, from F_{om} = 0.056 to F_{om} = 0.21 J cm^{-3} and reduces its R value from 9.3 to 5.7.

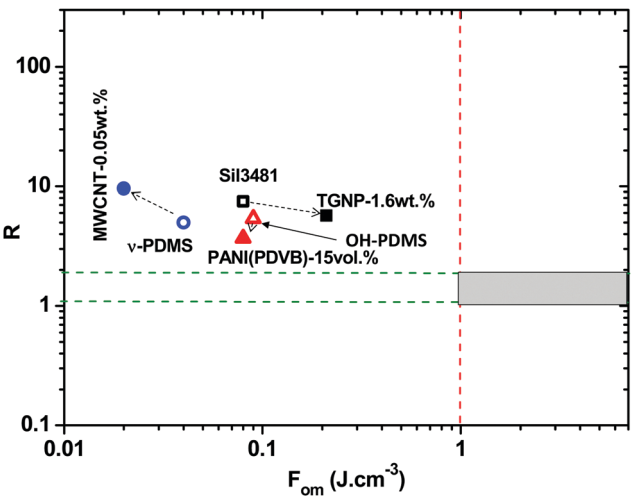

Fig. 12 Comparison between the F_{om} and R parameters of different unloaded elastomers (empty symbols) and loaded with conductive or core–shell charges (solid symbols).

Furthermore, polyaniline (PANI)-type particles encapsulated in divinylbenzene (DVB) *via* mini-emulsion polymerization have been included as fillers in a crosslinked PDMS matrix.[70] As expected, the PDMS/PANI(PDVB) composite reveals an increase in permittivity at 100 Hz from ε_r = 2.3 for the unloaded PDMS to ε_r = 3.3 for the PDMS loaded with 15 vol% fillers. However, the Young's modulus and the breakdown field decrease from Y = 0.48 MPa to 0.28 MPa, and from E_b = 66V μm^{-1} to 50.9 V μm^{-1}. Despite the increase in the dielectric constant and the possibility of incorporating a high filler content, the decrease in breakdown voltage results in a slight decrease in the figure of merit of this material compared with that of unloaded silicone (from E_d = 0.09 J cm^{-3} to 0.08 J cm^{-3}).

All these studies show that the addition of conductive fillers is an effective way to improve the dielectric constant of elastomer matrices, but their impact on other properties is highly variable and depends on many parameters. Even if certain authors have shown an improvement in the actuation performance when the dielectric elastomers are loaded with conductive particles, this bibliographic study revealed that it did not always concord with bringing materials close to the target domain for the application, as shown in Fig. 12.

3.2.2.2 Non-conducting fillers. Non-conducting fillers have also been introduced into elastomeric matrices. Compared to conductive fillers, they have the advantage of having a generally higher relative permittivity and of being non-conductive, and their proportion in the material is not limited by the percolation threshold. Thus, dispersion of inorganic fillers such as titanium dioxide (TiO_2),[38,72,73] barium titanate ($BaTiO_3$-BT)[61,74,75] or boron nitride (BN)[76] has often been reported. Table 6 presents the property changes for some PDMS elastomers that contain with such fillers.

Adding 30 wt% TiO_2 to Cine-Skin silicone increases its permittivity at 10 Hz from ε_r = 5.5 to 7.5,[63] while the Young's modulus and electrical breakdown strength are simultaneously decreased from Y = 0.04 to 0.016 MPa, and from E_b = 14.6 to 10 V μm^{-1}. Therefore, the figure of merit remains extremely low (F_{om} < 0.01 J cm^{-3}) despite the addition of a large amount of TiO_2 filler. Nevertheless, adding TiO_2 to Silastic 3481[38] increases the figure of merit from F_{om} = 0.08 to more than 0.13 J cm^{-3} and the R ratio decreases from 7.5 to less than 5.0. In detail, adding a filler results in an increase in the dielectric permittivity from ε_r = 3.6 to 6, an increase in the dielectric breakdown strength from E_b = 50 V μm^{-1} to E_b > 50 V μm^{-1} and the Young's modulus is almost unchanged (Y = 0.61 MPa and 0.67 MPa).

The use of high-dielectric-permittivity fillers such as calcium copper titanate ($CaCu_3Ti_4O_{12}$, or CCTO; $\varepsilon_r \approx 10^4$) has also been investigated.[40] The addition of 20 wt% CCTO to Blue Star PDMS increases its dielectric permittivity at 1 kHz from ε_r = 3.1 to 5.2, while not modifying its Young's modulus (0.38 MPa), although it divides the electrical breakdown strength by 2. The addition of $CaCu_3Ti_4O_{12}$ fillers leads to a decrease in the figure of merit of the composite (F_{om} = 0.035 J cm^{-3}) but also an increase of the R ratio to 11. Consequently, this composite is far from the target area.

Barium titanate ($BaTiO_3$, or BT) is another interesting type of filler to increase the dielectric permittivity of elastomers. The effects of the content (from 10 to 30 vol%) and the size (from 125 nm to 3 μm diameter) of these particles in composites based on Elastosil RT625 silicone have been investigated.[61] As a general behavior, the dielectric permittivity is increased by adding BT particles, from ε_r = 3 for pristine PDMS to more than 4.4 for a composite. Simultaneously, the Young's modulus is doubled for the composite containing 20 vol% BT (<2 μm). In addition, 10 wt% micro-fillers (2 μm) improve the dielectric permittivity better than 10 wt% nano-fillers (300 nm) (ε_r = 4.4 *versus* ε_r = 4.7). Drying the particles before their incorporation also slightly improves the dielectric permittivity (ε_r = 7.2 and $\varepsilon_r \approx$ 7.5 for 20 vol% BT (3 μm) undried and dried, respectively) and significantly impacts the dielectric breakdown strength (increasing E_b from 18 to 40 V μm^{-1}). Thus, the figure of merit of PDMS filled with 20 vol% BT *versus* pristine PDMS increases from F_{om} = 0.05 to 0.1 J cm^{-3} for dried particles while it decreases for non-dried fillers (F_{om} = 0.02 J cm^{-3}).

Vudayagiri *et al.*[34] investigated the effect of different proportions (3, 6 and 9 wt%) of commercially available fillers (anatase TiO_2, core–shell TiO_2–SiO_2, or $CaCu_3Ti_4O_2$) on the dielectric permittivity, modulus and electrical breakdown of various Elastosil silicones (LR3043, LR3005, and POWERSIL®XLR630). These effects depend on the nature of the elastomer/filler pair. The uniform dispersion of the filler with an appropriate concentration in the elastomer leads to an increase in the electromechanical properties. TiO_2 is the best candidate for

Table 6 Properties of different silicones modified by inorganic fillers. Values in bold type correspond to the unfilled elastomer

Silicone (commercial name)	Filler	Amount	ε_r	E_b (V μm^{-1})	Y (MPa)	F_{om} (J cm^{-3})	$R = Y/F_{om}$	Ref.
Cine-Skin[a]	**0**	**0**	**5.5**[e]	**14.6**	**0.04**[b]	**0.010**	**3.8**	63
	TiO_2 (10 μm)	30 wt%	7.5[e]	10	0.016[b]	0.007	2.4	
Silastic 3481	**N.S.**	**N.S.**	**3.6**[e]	**50**	**0.61**	**0.08**	**7.5**	38
	TiO_2 (3 μm)	30 phr	6[e]	>50	0.67	>0.13	<5.0	
Blue Star	**0**	**0**	**3.1**[f]	**55.9**	**0.37**	**0.09**	**4.3**	40
	CCTO (5 μm)	20 wt%	5.2[f]	27.4	0.38	0.035	11	
Elastosil RT625[c]	**0**	**0**	**3.0**[f]	**45**	**0.084**	**0.054**	**1.6**	61
	$BaTiO_3$ (<3 μm)	20 vol%	7.2[f]	18	0.17	0.021	8.2	
	$BaTiO_3$ (<3 μm) dried	20 vol%	7.5[f]	40	N.S.	0.106	—	
Elastosil LR3043/50	**0**	**0**	**2.8**[g]	**144**	**0.54**[d]	**0.51**	**1.0**	34
	TiO_2 (21 nm)	9 wt%	5.6[g]	141	0.30[d]	0.99	0.3	
Elastosil LR 3005/50	**0**	**0**	**2.9**[g]	**115**	**0.28**[d]	**0.34**	**0.8**	34
	TiO_2 (21 nm)	9 wt%	3.2[g]	136	0.22[d]	0.52	0.4	
XLR 630[c]	**0**	**0**	**2.9**[g]	**134**	**0.24**[d]	**0.46**	**0.5**	34
	TiO_2-SiO_2 Aeroxide	3 wt%	3.2[g]	108	0.29[d]	0.33	0.9	
		6 wt%	3.4[g]	173	0.19[d]	0.91	0.2	
		9 wt%	3.5[g]	126	0.30[d]	0.49	0.6	

N.S.: not specified. [a] PDMS tricomponent: 50 wt% PDMS/5 wt% hardener/45 wt% softener. [b] At 100% strain. [c] The commercial formula contains SiO_2 as an additive. [d] $Y = 3G'$. [e] At 10 Hz. [f] At 1 kHz. [g] At 0.1 Hz.

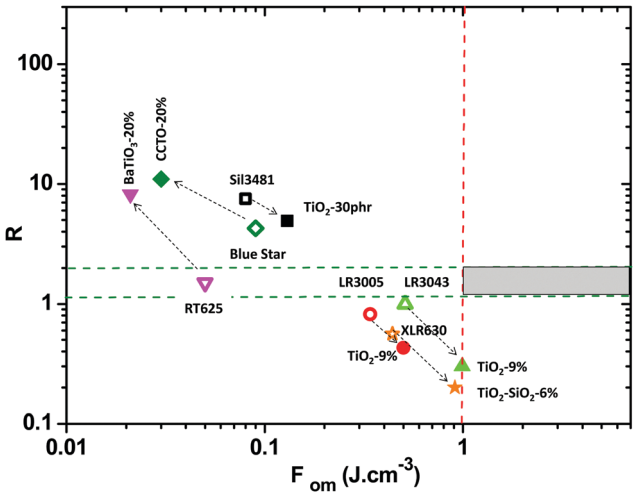

Fig. 13 Comparison between the F_{om} and R parameters of non-filled silicones (empty symbols) and of silicones filled with inorganic particles (full symbols).

increasing the dielectric permittivity, reaching, for example, $\varepsilon_{r\ 0.1Hz}$ = 5.6 for LR3043 with 9 wt% filler *versus* 2.8 without the filler. The core–shell TiO_2–SiO_2 filler improves the breakdown field. Thus, the highest value is obtained for XLR 630 silicone filled with 6 wt% core–shell TiO_2–SiO_2 (E_b = 173 V μm^{-1}). This filler/elastomer pair is also the most efficient for reinforcing the silicone's modulus from 0.24 MPa to 0.30 MPa with 9 wt% filler. In addition, the effect of fillers on the breakdown strength seems correlated with that of the effect on the Young's modulus. Finally, the same fillers can have opposite effects on the electromechanical properties, depending on the silicone matrix, making any prediction difficult (Fig. 13).

Other works on BT,[77] lead magnesium niobate–lead titanate (PMN–PT)[78] and lead zirconate titanate (PZT)[79] have demonstrated that the addition of ferroelectric ceramics is not systematically a good strategy for increasing the properties of the DEA. While an increase in the dielectric permittivity is described for all the fillers studied, the performance of the resulting DEA is not improved. The authors provide three explanations for this phenomenon: (i) an increase in the Young's modulus, (ii) a decrease in the dielectric breakdown strength, and (iii) an increase in the dielectric losses.

In summary, the addition of inorganic fillers is an efficient strategy to increase the dielectric permittivity of elastomers. However, the effect on the dielectric breakdown strength (either an increase or a decrease) depends on the considered system. Therefore, the incorporation of fillers can raise or lower the figure of merit and the R ratio (Fig. 13).

3.2.3 Addition of plasticizers. The simplest solution to modify the mechanical properties of a polymer is to plasticize it, *i.e.*, to introduce a plasticizer which decreases the inter/intramolecular interactions between the macromolecules. Thus, the Young's modulus is generally lowered and the deformation is eased. This strategy was applied to nitrile butadiene rubber (NBR) by adding dioctylphthalate (DOP),[80] which decreases the elastic modulus from 1.3 to 0.34 MPa, and consequently increases the radial deformation at 20 V μm^{-1} from 0.13 to 1.6%. Otherwise, the effect of epoxidized soybean oil as a plasticizer on the dielectric and mechanical properties of hydrogenated NBR (HNBR), either filled or not with 40 wt% TiO_2, was studied.[28] The incorporation of 30 wt% oil slightly decreases the dielectric permittivity (from ε_r = 12.5 to 11.5) and the elastic modulus (from Y = 1.6 to 0.75 MPa) of the HNBR matrix. Thus, the actuation at 30 V μm^{-1} is increased by 100% compared with the non-plasticized HNBR matrix. The addition of 30 wt% oil to a 40 wt% TiO_2/HNBR composite also weakens the interaction between the HNBR and the fillers, which further increases the actuation, by 170% at 30 V μm^{-1} compared with the 40 wt% TiO_2/HNBR composite.

The addition of a plasticizer to filled or unfilled elastomers can thus be an efficient solution to improve the actuation. However, these small molecules are not linked to the matrix and they can therefore easily migrate, which constitutes a major drawback to their stability over time and thus their use in different applications.

After this non-exhaustive review of the different possibilities of modifying the electromechanical properties of dielectric elastomers by adding an exogenous component, the different pathways of chemical modifications of elastomers which have been tested in the literature are now presented.

3.3 Elastomer chemical modifications

In this part, unlike in the previous examples, the molecular structure of the elastomers is irreversibly changed.[9,81,82] The elastomer structure can be modified during its synthesis by increasing the crosslinking density (elastic behavior), by introducing pendant chains (free volume) or polar grafted chains (increasing the material's polarity), or by tuning the gel fraction (viscous behavior). These modifications thus tune the electromechanical behavior of the dielectric elastomer.

3.3.1 Crosslinking density and crosslinker nature. Some examples of the effect of the crosslinking density and the crosslinker nature on the characteristics of elastomers are detailed in Table 7.

The crosslinking density of a silicone elastomer synthesized *via* polycondensation can be modified by varying the proportions of both components, as shown with a Dow Corning silicone (DC 3481) reacting with increasing amounts of crosslinking agent (hardener: 81-R from Suter-Kunstsoffe). Thus, the Young's modulus and the breakdown field increase with the crosslinking density while the dielectric constant of the materials is unchanged.[83] More precisely, adding from 5 to 40 wt% crosslinker causes an increase of 50% in the Young's modulus (from Y = 0.35 to 0.52 MPa) and 76% in the breakdown field (from E_b = 41 to 72 V μm^{-1}), while the dielectric permittivity remains constant (ε_r = 3.2). Moreover, the permittivity can be improved from ε_r = 3.2 to $\varepsilon_r \approx$ 3.7 by modifying the nature of the crosslinker (by substituting of 81-R with 81-F or 81-VF (from the same manufacturer)). Simultaneously, the Young's modulus also increases from Y = 0.35 with 81-R to 0.43 MPa and 0.56 MPa with 81-F and 81-VF, respectively. The chemical nature of these crosslinkers has not been identified and thus it was not possible to establish a structure–property relationship. This work

Table 7 Influence of crosslinking density and crosslinker nature on the electromechanical properties of elastomers. Values in bold type correspond to the parent elastomer

Polymer	Crosslinker	ε_r	E_b (V μm^{-1})	Y (MPa)	F_{om} (J cm^{-3})	$R = Y/F_{om}$	Ref.
Silicone DC 3481	5 wt% 81-R	3.25	41	0.35	0.05	7.2	83
	10 wt% 81-R	3.24	61	0.49	0.11	4.6	
	20 wt% 81-R	3.21	66	0.51	0.12	4.1	
	40 wt% 81-R	3.20	72	0.52	0.15	3.5	
	5 wt% 81-F	3.73	62	0.43	0.13	3.4	
	5 wt% 81-VF	3.68	71	0.56	0.16	3.4	
Co-polyacrylate	**0 wt%**	**5**	**114**	**2.46**	**0.58**	**4.3**	84
	5 wt% HDDA	4.9	236	4.38	2.42	1.8	

shows that the actuation properties can be improved by adjusting the modulus and the permittivity. Globally the increase in the breakdown field can increase the figure of merit of DC 3481 by a factor of 3, from 0.05 to 0.16, and, since the Young's modulus increases slightly, the R ratio is concomitantly divided by 2 (from 7.2 to 3.4). However, these materials remain far from the desired target area (Fig. 14). Similar results on the crosslinking density of an elastomer have been observed for a polyacrylate network.[84] Thus, when a 5 wt% crosslinking agent, 1,6-hexanedioldiacrylate (HDDA), is added to an acrylate-based network during its synthesis, the permittivity remains constant ($\varepsilon_r \approx$ 5–4.9) while the Young's modulus and the breakdown strength are doubled. The authors thus succeeded in mastering the stress–strain relationship without modifying the dielectric constant and, in addition, suppressed the electromechanical instability. Very high actuation strains have been obtained without prestrain despite an increase in Young's modulus. This improvement has allowed the material to move into the defined target area with a figure of merit F_{om} = 2.42 J cm^{-3} and an R ratio = 1.8.

These studies show that the amount and nature of the elastomer cross-linkers have a significant impact on the electromechanical properties.

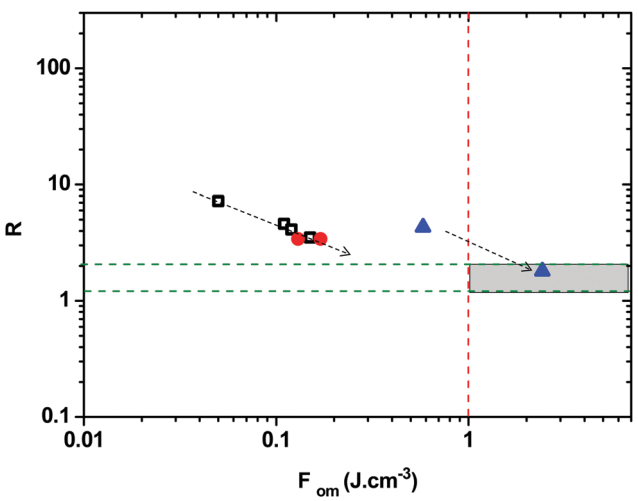

Fig. 14 Comparison between the F_{om} and R parameters of a silicone elastomer (empty squares) according to the crosslinking density, and for a silicone elastomer (full circles) and a polyacrylate elastomer (full triangles) according to the crosslinker nature.

3.3.2 Addition of functional groups. Another pathway consists of adding functional groups to the polymer chains to vary the properties of the materials and their electromechanical response. Functional groups can be added either at the time of synthesis, or *via* post-processing. Hydrosilylation, the main reaction used for silicone crosslinking and the grafting of functional groups, as well as the structure of some functionalized elastomer networks modified in this way as well as the chemical formula of some precursors are represented in Fig. 15. The characteristics of elastomers containing functional groups are summarized in Table 8.

For instance, vinyl (–Si–CH=CH$_2$) telechelic PDMS (DMS-V31) is crosslinked *via* hydrosilylation with hydrosilane (–Si–H) units of crosslinker (HMS-301). These silicones have been modified by grafting *N*-allyl-*N*-methyl-*p*-nitroaniline (NANMPN) *via* hydrosilylation on some silane ends. The addition of NANMPN is interesting due to its dipolar character, which allows the silicone permittivity to be increased while simultaneously reducing the crosslinking density, and therefore the material's modulus.[81,82,85] Consequently, the dielectric permittivity is increased from ε_r = 3 to ε_r = 6.0, and the Young's modulus is decreased from Y = 1.9 MPa to 0.55 MPa when 13.4 wt% NANMPN is enclosed. However, the introduction of a dipole moment reduces the breakdown field from E_b = 129 to 40 V μm^{-1}. Thus, these variations decrease the figure of merit by about a factor of 5 (0.44 J cm^{-3} for pure DMS-V31 and 0.08 J cm^{-3} for modified DMS-V31) and increase the R ratio (from 4.3 to 6.5). Similar trends are observed when Elastosil RT625 or Sylgard 184 silicones are modified with 10.7 wt% NANMPN grafts: the dielectric permittivity increases, and the Young's modulus and breakdown field decrease to different extents, leading to a decrease in the figure of merit and an increase in R ratio for Elastosil RT625 but a decrease in both factors in Sylgard 184 (Table 8).[81] Finally, although the dielectric permittivity of these three silicones was increased when between 10.7 and 13.4 wt% NANMPN was added, the modified materials were moved further away from the target area (Fig. 16). In another study the authors used crosslinkers to introduce the dipolar functional groups in a PDMS network.[86] This study shows that the use of crosslinkers 2 and 5 (Fig. 15) with polar functional groups also increases the permittivity (from 2.8 to 3.2). In the case of crosslinker 5 the breakdown field is increased slightly from 111 to 124 V μm^{-1} while it decreases with crosslinker 2, as reported for the other chemical

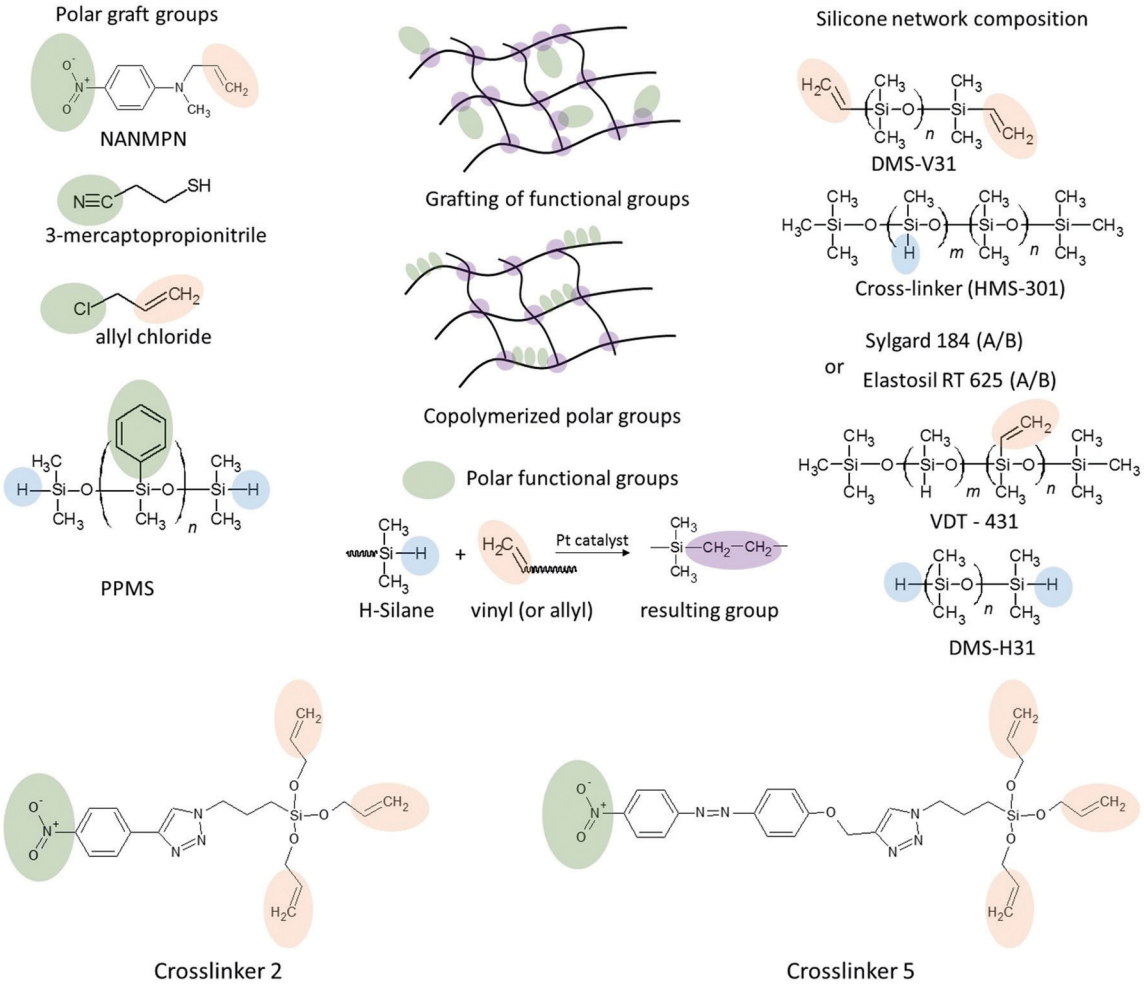

Fig. 15 Addition of functional groups on silicone networks.

Table 8 Properties of different silicone elastomers chemically modified. Values in bold type correspond to the unmodified elastomer

Elastomer	Graft/block	Graft content	ε_r	E_b (V μm^{-1})	Y (MPa)	F_{om} (J cm^{-3})	$R = Y/F_{om}$	Ref.
DMS-V31 (DMS-V31)	**0**	**0**	**3**[a]	**129**	**1.9**	**0.44**	**4.3**	82
	NANMPN	13.4 wt%	6.0[a]	40	0.55	0.08	6.5	
Sylgard 184 (Sil184)	**0**	**0**	**2.84**[a]	**118**	**2.5**	**0.35**	**7.1**	81
	NANMPN	10.7 wt%	6.15[a]	61.1	0.85	0.20	4.2	
Elastosil RT625 (RT625)	**0**	**0**	**3.17**[a]	75	**0.3**	**0.16**	**1.9**	81
	NANMPN	10.7 wt%	5.56[a]	30.7	0.14	0.05	3.0	
Silicone DMS-H21/VDT-431 (DMS-H21)	**0**	**0**	**2.8**	**111**	**0.54**	**0.31**	**1.8**	86
	Crosslinker 5	1.35 wt%	3.2	124.2	0.15[a]	0.44	0.3	
	Crosslinker 2	1.35 wt%	3.3	91.9	0.45[a]	0.24	1.8	
Crosslinked PDMS	**0**	**0**	**2.8**[b]	**N.S.**	**0.07**	—	—	87
	3-Mercaptopropionitrile	N.S.	10.1[b]	10.8	0.154	0.01	14.7	
PHMS-*g*-PDMS	Allyl chloride	16.1 mol%	4.7[c]	94.4	1	0.37	2.7	9
PDMS crosslinked with DMS-H31 (PDMS)	**0**	**0**	**3.7**[d]	**53**	**0.31**	**0.09**	**3.37**	88
	PPMS[x] (block)	8.4×10^{-4} (mol g^{-1})	3.7[d]	72	0.45	0.17	2.7	
	PPMS[y] (block)	20×10^{-4} (mol g^{-1})	3.4[d]	56	0.27	0.09	2.9	

N.S.: not specified. [a] At 1 kHz. [b] At 10 kHz. [c] At 100 Hz. [d] At 1 Hz.

functionalization with dipolar nitro groups. The use of both crosslinkers results in a decrease in the Young's moduli with a varying magnitude depending on the crosslinker. In this work the increase in the dielectric permittivity is not enough to increase the energy density of the materials (F_{om}) up to the target area.

Silicones have also been modified with other polar moieties. For instance, modification with nitrile groups by grafting

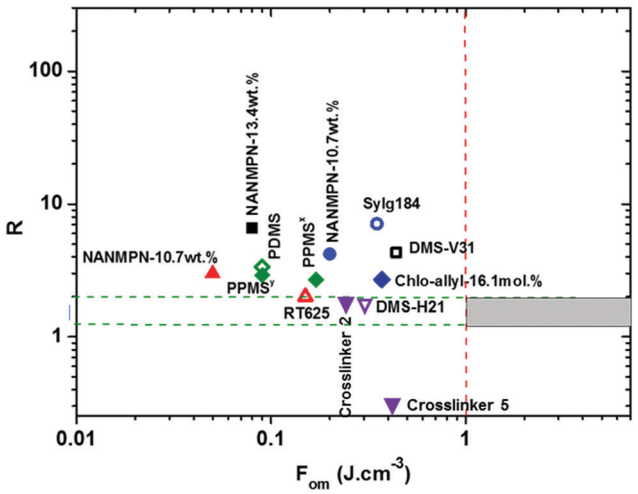

Fig. 16 Comparison between the F_{om} and R parameters of unmodified silicones (empty symbols) and silicones grafted with different polar groups (full symbols).

3-mercaptopropionitrile on a silicone network increases its permittivity from ε_r = 2.8 to 10.1 (at 10^4 Hz). By using an appropriate crosslinker content and silica charge, it is possible to adjust the final mechanical properties of the matrix and the Young's modulus from Y = 0.07 to 0.154 MPa.[87] This material shows an interesting self-healing capacity after breakdown at low actuation voltages. However, due to its low breakdown field, the resulting material is located quite far from the target area. Another example is given with the grafting of allyl chloride, which also improves the electromechanical properties of the silicone.[9] A PHMS-*g*-PDMS (HS6) elastomer was modified with 16.1 mol% allyl chloride grafts and this new material has a high average permittivity (ε_r = 4.7), a high breakdown field (E_b = 94.4 V μm^{-1}), and a low elastic modulus (Y = 1 MPa), which locate it in the vicinity of the target area (F_{om} = 0.37; $R = Y/F_{om}$ = 2.7) (Fig. 16).

Elastomers have also been chemically modified to increase the breakdown field by incorporating groups that are resistant to high voltages. For instance, phenyl substituents are good at stabilizing silicones because the delocalized π electrons trap the kinetic electrons generated by the electric field.[88] Thus, crosslinked block PDMS–PPMS (polydimethylsiloxane–polyphenylmethylsiloxane) copolymers with different proportions of phenyl groups show the relative permittivity varying slightly with the phenyl group concentration but an increase of up to 36% in the breakdown field (reaching 72 ± 3 V μm^{-1}) compared with a PDMS without phenyl substituents. In addition, phenyl-containing blocks do not rigidify the copolymers, thus their modulus remains close to that of PDMS (Y = 0.31 MPa). The figure of merit and the Y/F_{om} ratio of the PDMS containing 8.4 × 10^{-4} mol g^{-1} phenyl groups are closer to the target area since the figure of merit increases from F_{om} = 0.09 to 0.17 J cm^{-3}, and the Y/F_{om} ratio decreases from 3.37 to 2.7. The introduction of polar groups and/or phenyl groups therefore appears to be effective in changing the elastomer properties and making them tend towards the target area, and as a consequence further to this work this area has been investigated.[89,90]

4. Discussion

In summary, numerous strategies have been explored to improve the electromechanical properties of DEAs. While the use of $R = f(F_{om})$ charts appears to be a rational and powerful way to compare the materials, the review work also highlights the strong interdependency of the three electromechanical properties that must be considered: the breakdown field (E_b), the relative permittivity (ε_r) and the Young's modulus (Y). The choice of one strategy to improve one of these properties usually has a strong impact on at least one of the other properties and makes it difficult to predict its effects on the overall performance.

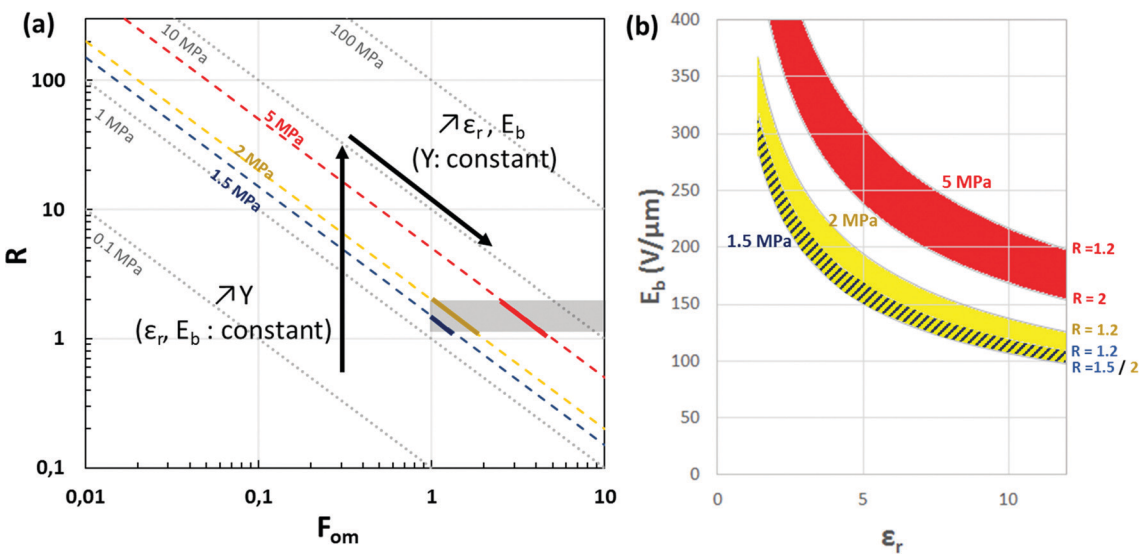

Fig. 17 (a) *R vs.* F_{om} charts as tool to predict the electromechanical properties for targeting. (b) Area defining the targeted value couples of E_b and ε_r for three different Young's modulus values (blue stripes, Y = 1.5 MPA; yellow, Y = 2 MPa; and red, Y = 5 MPa).

However, the comparison approach described here can be used to guide the scientist in the determination of target properties. First, the Young's modulus must be considered. Most of the research on the synthesis and modification of dielectric elastomers usually targets a low Young's modulus at first, aiming at increasing the Maxwell-pressure-induced strain. However, the effective work of the resulting artificial muscle might be too low for practical applications. Knowing that $R = \frac{Y}{\varepsilon_0 \varepsilon_r E_b^2}$ and $F_{om} = \varepsilon_0 \varepsilon_r E_b^2$, the log–log plot of $R = f(F_{om})$ can provide useful and counterintuitive information on this matter by drawing the typical lines along which materials of the same Y value line up (Fig. 17a). Without considering the dielectric permittivity and electrical breakdown strength, materials with a Young's modulus below 1.2 MPa never reach the target area. Therefore, targeting only an increase in the Young's modulus of the DE can be interesting, but the positioning of the material is simply shifted upward and further away from the target area. Second, by increasing ε_r and/or E_b, the position of the material is shifted along the Young's modulus line and specific couples of values ε_r and E_b can consequently be targeted. The points on the blue, yellow and red segments (Fig. 17a) within the target area correspond to examples of such materials, with defined Young's moduli and with suitable values of ε_r and E_b. These value couples can be visualized as areas in an $E_b = f(\varepsilon_r)$ plot as reported in Fig. 17b. It appears to become possible for one defined Young's modulus to target specifically a necessary breakdown strength when the dielectric permittivity is known, or *vice versa*. One can also see that materials with a Young's modulus as high as 5 MPa can be suitable for practical applications, providing that the dielectric permittivity and breakdown strength values are appropriate.

This rational comparison method can thus be used as a tool to guide chemists, physicists and engineers to develop the ideal materials and to turn them into innovative applications.

Conclusion

This state of the art on dielectric elastomers for actuators allowed the compilation of the dielectric permittivities, Young's moduli, and breakdown fields of a hundred materials. The various methods to improve the elastomer properties and their effects were then screened. The trends identified can be used to choose the most suitable procedure to obtain the desired elastomer. Thus, prestretching the sample mainly allows the breakdown voltage to be increased. The addition of a filler increases the elastomer permittivity and has a variable impact on other properties depending on many parameters. The impact of this modification on the mechanical properties is difficult to predict, with a lack of data on the viscoelastic and hysteresis properties of the mechanical responses. The cross-linking density of networks allows control over the Young's modulus, and potentially improves the breakdown field. The increase in the breakdown field and/or permittivity can be controlled by grafting polar molecules or the phenyl structure on elastomers. However, these modifications often lead to the desired effects on some properties, but to the reverse on others, which is why a methodology for classifying the different polymer materials according to their actuation efficiency has been proposed.

The figure of merit, $F_{om} = \varepsilon_0 \varepsilon_r E_b^2$, and the ratio, $R = \frac{Y}{F_{om}}$, have been chosen as suitable parameters to analyze the compromise that should be found between the electric field, the relative permittivity and the Young's modulus. Thus, the energy density of any dielectric polymer increases with F_{om} while the ratio R should be kept higher than 1, to guarantee a stable polymer until electrical breakdown, and should not exceed 2, in order to have a soft material. Thus, for instance, among the available materials, silicone Nusil CF21-1986, and polyurethanes Bayfol EA102 and TPU-LPT4210-UT50 are qualified for these defined criteria.

Finally, the study on the evolution of the F_{om} and R parameters according to the 3 main properties of materials (dielectric permittivity, Young's modulus, and breakdown field) shows that it is necessary to have an initial material with a Young's modulus that is high enough to be able to hope to reach the target area when modifying the other two properties (dielectric permittivity and breakdown field).

Conflicts of interest

There are no conflicts of interest to declare.

References

1 F. Carpi, D. De Rossi, R. Kornbluh, R. Pelrine and P. Sommer-Larsen, *Dielectric elastomers as electromechanical transducers: Fundamentals, Materials, Devices, Models and Applications of an Emerging Electroactive Polymer Technology. Dielectric Elastomers as Electromechanical Transducers*, Elsevier, 2008, p. 329.

2 Y. Bar-Cohen, Electroactive Polymer (EAP) Actuators as Artificial Muscles: Reality, Potential, and Challenges, *Electroactive Polymer (EAP) Actuators as Artificial Muscles: Reality, Potential, and Challenges*, 2nd edn, 2004.

3 S. Soulimane, Conception et modélisation d'un micro-actionneur à base d'élastomère diélectrique, *Université Toulouse III*, Paul Sabatier, 2010.

4 S. Hau, High-Performance Dielectric Elastomer Actuators. 2018.

5 D. F. Hanson, G. Pioggia, Y. Bar-Cohen and D. de Rossi, Androids: application of EAP as artificial muscles to entertainment industry, *Smart Struct Mater 2001 Electroact Polym Actuators Devices*, 2001, **4329**, 375.

6 L. J. Romasanta, M. A. Lopez-Manchado and R. Verdejo, Increasing the performance of dielectric elastomer actuators: A review from the materials perspective, *Prog. Polym. Sci.*, 2015, **51**, 188–211, DOI: 10.1016/j.progpolymsci.2015.08.002.

7 T. Lu, C. Ma and T. Wang, Mechanics of dielectric elastomer structures: A review, *Ext. Mech. Lett.*, 2020, **38**, 100752, DOI: 10.1016/j.eml.2020.100752.

8 R. Pelrine, R. Kornbluh, Q. Pei and J. Joseph, High-speed electrically actuated elastomers with strain greater than 100%, *Science*, 2000, **287**(5454), 836–839.
9 F. B. Madsen, A. E. Daugaard, S. Hvilsted and A. L. Skov, The Current State of Silicone-Based Dielectric Elastomer Transducers, *Macromol. Rapid Commun.*, 2016, **37**(5), 378–413.
10 A. L. Skov and L. Yu, Optimization Techniques for Improving the Performance of Silicone-Based Dielectric Elastomers, *Adv. Eng. Mater.*, 2018, **20**(5), 1–21.
11 P. Mazurek, S. Vudayagiri and A. L. Skov, How to tailor flexible silicone elastomers with mechanical integrity: a tutorial review, *Chem. Soc. Rev.*, 2019, **48**(6), 1448–1464.
12 C. Tugui, G. T. Stiubianu, M. S. Serbulea and M. Cazacu, Silicone dielectric elastomers optimized by crosslinking pattern-a simple approach to high-performance actuators, *Polym. Chem.*, 2020, **11**(19), 3271–3284, DOI: 10.1039/D0PY00223B.
13 J. Huang, S. Shian, R. M. Diebold, Z. Suo and D. R. Clarke, The thickness and stretch dependence of the electrical breakdown strength of an acrylic dielectric elastomer, *Appl. Phys. Lett.*, 2012, **101**, 122905.
14 J. Diani, B. Fayolle and P. Gilormini, A review on the Mullins effect, *Eur. Polym. J.*, 2009, **45**(3), 601–612, DOI: 10.1016/j.eurpolymj.2008.11.017.
15 M. Huang, L. B. Tunnicliffe, J. Zhuang, W. Ren, H. Yan and J. J. C. Busfield, Strain-Dependent Dielectric Behavior of Carbon Black Reinforced Natural Rubber, *Macromolecules*, 2016, **49**(6), 2339–2347.
16 Z. Suo, Theory of dielectric elastomers, *Acta Mech. Solida Sin.*, 2010, **23**(6), 549–578.
17 R. W. Ogden, Large deformation isotropic elasticity – on the correlation of theory and experiment for incompressible rubberlike solids, *Proc. R. Soc. London, Ser. A*, 1972, **326**(1567), 565–584.
18 O. H. Yeoh, Some forms of the strain energy function for rubber, *Rubber Chem. Technol.*, 1993, **66**(5), 754–771.
19 L. Mullins, in *Engineering With Rubber*, ed. Hanse, Chemtech, 3rd edn, 1987, pp. 720–727.
20 N. Della Schiava, K. Thetpraphi, M. Q. Le, P. Lermusiaux, A. Millon and J. F. Capsal, *et al.*, Enhanced figures of merit for a high-performing actuator in electrostrictive materials, *Polymers*, 2018, **10**(3), 263.
21 X. Zhao and Z. Suo, Theory of dielectric elastomers capable of giant deformation of actuation, *Phys. Rev. Lett.*, 2010, **104**(17), 178302.
22 J. Chavanne Cylindrical Dielectric Elastomer Actuator for Cardiac Assist Device Thèse No 9397 Jonathan André Jean-Marie CHAVANNE, 2019, 168, available from: http://infoscience.epfl.ch/record/265412.
23 S. I. Rich, R. J. Wood and C. Majidi, Untethered soft robotics, *Nat Electron.*, 2018, **1**(2), 102–112.
24 S. J. A. Koh, C. Keplinger, T. Li, S. Bauer and Z. Suo, Dielectric elastomer generators: How much energy can be converted?, *IEEE/ASME Trans. Mechatronics*, 2011, **16**(1), 33–41.
25 G. Kofod, R. D. Kornbluh, R. Pelrine and P. Sommer-Larsen, Actuation response of polyacrylate dielectric elastomers, in *Smart Structures and Materials*, ed. Y. Bar-Cohen, Electroactive Polymer Actuators and Devices, 2001, p. 141.
26 R. E. Pelrine, R. D. Kornbluh and J. P. Joseph, Electrostriction of polymer dielectrics with compliant electrodes as a means of actuation, *Sens. Actuators, A*, 1998, **64**(1), 77–85.
27 J. Biggs, K. Danielmeier, J. Hitzbleck, J. Krause, T. Kridl and S. Nowak, *et al.*, Electroactive polymers: Developments of and perspectives for dielectric elastomers, *Angew. Chem., Int. Ed.*, 2013, **52**, 9409–9421.
28 D. Yang, L. Zhang, N. Ning, D. Li, Z. Wang and T. Nishi, *et al.*, Large increase in actuated strain of HNBR dielectric elastomer by controlling molecular interaction and dielectric filler network, *RSC Adv.*, 2013, **3**(44), 21896–21904.
29 R. Pelrine, R. Kornbluh, J. Joseph, R. Heydt, Q. Pei and S. Chiba, High-field deformation of elastomeric dielectrics for actuators, 2000.
30 D. Yang, M. Tian, Y. Dong, H. Liu, Y. Yu and L. Zhang, Disclosed dielectric and electromechanical properties of hydrogenated nitrile-butadiene dielectric elastomer, *Smart Mater. Struct.*, 2012, **21**(3), 035017.
31 C. Ellingford, C. Bowen, T. McNally and C. Wan, Intrinsically Tuning the Electromechanical Properties of Elastomeric Dielectrics: A Chemistry Perspective, *Macromolecular Rapid Communications*, Wiley-VCH Verlag, 2018, vol. 39.
32 R. Shankar, T. K. Ghosh and R. J. Spontak, Electromechanical response of nanostructured polymer systems with no mechanical pre-strain, *Macromol. Rapid Commun.*, 2007, **28**(10), 1142–1147.
33 L. Petit, B. Guiffard, L. Seveyrat and D. Guyomar, Actuating abilities of electroactive carbon nanopowder/polyurethane composite films, *Sens. Actuators, A*, 2008, **148**(1), 105–110.
34 S. Vudayagiri, S. Zakaria, L. Yu, S. S. Hassouneh, M. Benslimane and A. L. Skov, High breakdown-strength composites from liquid silicone rubbers, *Smart Mater. Struct.*, 2014, **23**(10), 105017.
35 A. G. Wacker Chemie, NEW HORIZONS THROUGH INNOVATIVE APPLICATIONS WITH ELASTOSIL® FILM - ULTRA-THIN SILICONE FILM FOR HIGH-PRECISION SOLUTIONS - 7091e/09.16 reprint 7091e/04.16, 2020.
36 P. Lotz, M. Matysek, P. Lechner, M. Hamann and H. F. Schlaak, Dielectric elastomer actuators using improved thin film processing and nanosized particles, *Electroact Polym. Actuators Devices*, 2008, **6927**, 692723.
37 A. L. Skov, S. Vudayagiri and M. Benslimane, Novel silicone elastomer formulations for DEAPs, *Electroactive Polymer Actuators and Devices (EAPAD)*, SPIE, 2013, p. 86871I.
38 H. Liu, L. Zhang, D. Yang, Y. Yu, L. Yao and M. Tian, Mechanical, dielectric, and actuated strain of silicone elastomer filled with various types of TiO_2, *Soft Mater.*, 2013, **11**(3), 363–370.
39 S. Iglesias, *Composites conducteurs polymères hautement déformables pour la récupération d'énergie houlomotrice*, Université de Lyon, 2018.
40 L. J. Romasanta, P. Leret, L. Casaban, M. Hernández, M. A. De La Rubia and J. F. Fernández, *et al.*, Towards materials with enhanced electro-mechanical response:

$CaCu_3Ti_4O_{12}$-polydimethylsiloxane composites, *J. Mater. Chem.*, 2012, **22**(47), 24705–24712.

41 H. Sun, C. Jiang, N. Ning, L. Zhang, M. Tian and S. Yuan, Homogeneous dielectric elastomers with dramatically improved actuated strain by grafting dipoles onto SBS using thiol-ene click chemistry, *Polym. Chem.*, 2016, **7**(24), 4072–4080.

42 H. Stoyanov, M. Kollosche, S. Risse, D. N. McCarthy and G. Kofod, Elastic block copolymer nanocomposites with controlled interfacial interactions for artificial muscles with direct voltage control, *Soft Matter*, 2011, **7**(1), 194–202.

43 H. Stoyanov, D. Mc Carthy, M. Kollosche and G. Kofod, Dielectric properties and electric breakdown strength of a subpercolative composite of carbon black in thermoplastic copolymer, *Appl. Phys. Lett.*, 2009, **94**(23), 232905.

44 R. M. Grigorescu, F. Ciuprina, P. Ghioca, M. Ghiurea, L. Iancu and B. Spurcaciu, *et al.*, Mechanical and dielectric properties of SEBS modified by graphite inclusion and composite interface, *J. Phys. Chem. Solids*, 2016, **89**, 97–106.

45 R. D. Kornbluh, R. Pelrine, Q. Pei, S. Oh and J. Joseph, Ultrahigh strain response of field-actuated elastomeric polymers, *Smart Struct Mater 2000 Electroact Polym Actuators Devices*, 2000, **3987**, 51.

46 C. Tugui, S. Vlad, M. Iacob, C. D. Varganici, L. Pricop and M. Cazacu, Interpenetrating poly(urethane-urea)–polydimethylsiloxane networks designed as active elements in electromechanical transducers, *Polym. Chem.*, 2016, **7**(15), 2709–2719.

47 M. Wissler and E. Mazza, Electromechanical coupling in dielectric elastomer actuators, *Sens. Actuators, A*, 2007, **138**, 384–393.

48 J. Qiang, H. Chen and B. Li, Experimental study on the dielectric properties of polyacrylate dielectric elastomer, *Smart Mater. Struct.*, 2012, **21**(2), 025006.

49 W. Lai, *Characteristics of dielectric elastomers and fabrication of dielectric elastomer actuators for artificial muscle applications*, Master thesis, Iowa State University, 2011.

50 J. S. Plante and S. Dubowsky, Large-scale failure modes of dielectric elastomer actuators, *Int. J. Solids Struct.*, 2006, **43**(25–26), 7727–7751.

51 H. R. Choi, K. Jung, N. H. Chuc, M. Jung, I. Koo and J. Koo, *et al.*, Effects of prestrain on behavior of dielectric elastomer actuator, *Smart Structures and Materials 2005: Electroactive Polymer Actuators and Devices (EAPAD)*, SPIE, 2005, p. 283.

52 G. Kofod, The static actuation of dielectric elastomer actuators: How does pre-stretch improve actuation?, *J. Phys. D: Appl. Phys.*, 2008, **41**(21), 215405.

53 S. Akbari, S. Rosset and H. R. Shea, Improved electromechanical behavior in castable dielectric elastomer actuators, *Appl. Phys. Lett.*, 2013, **102**(7), 071906.

54 F. Carpi, G. Gallone, F. Galantini and D. De Rossi, Silicone-poly(hexylthiophene) blends as elastomers with enhanced electromechanical transduction properties, *Adv. Funct. Mater.*, 2008, **18**(2), 235–241.

55 G. Gallone, F. Galantini and F. Carpi, Perspectives for new dielectric elastomers with improved electromechanical actuation performance: Composites versus blends, *Polym. Int.*, 2010, **59**(3), 400–406.

56 A. H. A. Razak, P. Szabo and A. L. Skov, Enhancement of dielectric permittivity by incorporating PDMS-PEG multiblock copolymers in silicone elastomers, *RSC Adv.*, 2015, **5**(65), 53054–53062.

57 S. M. Ha, I. S. Park, M. Wissler, R. Pelrine, S. Stanford and K. J. Kim, *et al.*, High electromechanical performance of electroelastomers based on interpenetrating polymer networks, *Electroact Polym. Actuators Devices*, 2008, **6927**, 69272C.

58 L. Yu, F. B. Madsen, S. Hvilsted and A. L. Skov, High energy density interpenetrating networks from ionic networks and silicone. in *Electroactive Polymer Actuators and Devices (EAPAD)*, ed. Y. Bar-Cohen, SPIE, 2015, p. 94300T.

59 D. Yang, M. Ruan, S. Huang, Y. Wu, S. Li and H. Wang, *et al.*, Dopamine and silane functionalized barium titanate with improved electromechanical properties for silicone dielectric elastomers, *RSC Adv.*, 2016, **6**(93), 90172–90183.

60 D. Yang, F. Ge, M. Tian, N. Ning, L. Zhang and C. Zhao, *et al.*, Dielectric elastomer actuator with excellent electromechanical performance using slide-ring materials/barium titanate composites, *J. Mater. Chem. A*, 2015, **3**(18), 9468–9479.

61 H. Böse, D. Uhl, K. Flittner and H. Schlaak, Dielectric elastomer actuators with enhanced permittivity and strain. in *Electroactive Polymer Actuators and Devices (EAPAD)*, ed. Y. Bar-Cohen and F. Carpi, 2011, p. 79762J.

62 H. Stoyanov, P. Brochu, X. Niu, E. Della Gaspera and Q. Pei, Dielectric elastomer transducers with enhanced force output and work density, *Appl. Phys. Lett.*, 2012, **100**(26), 262902.

63 F. Carpi and D. de Rossi, Improvement of electromechanical actuating performances of a silicone dielectric elastomer by dispersion of titanium dioxide powder, *IEEE Trans. Dielectr. Electr. Insul.*, 2005, **12**(4), 835–843.

64 S. Priya and D. J. Inman, Energy harvesting technologies, *Energy Harvest Technol.*, 2009, 1–517.

65 M. Tian, Z. Wei, X. Zan, L. Zhang, J. Zhang and Q. Ma, *et al.*, Thermally expanded graphene nanoplates/polydimethylsiloxane composites with high dielectric constant, low dielectric loss and improved actuated strain, *Compos. Sci. Technol.*, 2014, **99**(27), 37–44.

66 L. J. Romasanta, M. Hernández, M. A. López-Manchado and R. Verdejo, Functionalised graphene sheets as effective high dielectric constant fillers, *Nanoscale Res. Lett.*, 2011, **6**, 1–6.

67 A. Egede Daugaard, S. S. Hassouneh, M. Kostrzewska, A. G. Bejenariu and A. L. Skov, High-dielectric permittivity elastomers from well-dispersed expanded graphite in low concentrations, *Electroact Polym Actuators Devices*, 2013, **8687**, 868729.

68 S. K. Yadav, I. J. Kim, H. J. Kim, J. Kim, S. M. Hong and C. M. Koo, PDMS/MWCNT nanocomposite actuators using silicone functionalized multiwalled carbon nanotubes via nitrene chemistry, *J. Mater. Chem. C*, 2013, **1**(35), 5463–5470.

69 R. R. Kohlmeyer, A. Javadi, B. Pradhan, S. Pilla, K. Setyowatt and J. Chen, *et al.*, Electrical and dielectric properties

of hydroxylated carbon nanotube-elastomer composites, *J. Phys. Chem. C*, 2009, **113**(41), 17626–17629.

70 M. Molberg, D. Crespy, P. Rupper, F. Nüesch, J. A. E. Manson and C. Löwe, *et al.*, High breakdown field dielectric elastomer actuators using encapsulated polyaniline as high dielectric constant filler, *Adv. Funct. Mater.*, 2010, **20**(19), 3280–3291.

71 T. J. Lewis, Interfaces are the dominant feature of dielectrics at the nanometric level, *IEEE Trans. Dielectr. Electr. Insul.*, 2004, **11**(5), 739–753.

72 M. Razzaghi Kashani, S. Javadi and N. Gharavi, Dielectric properties of silicone rubber-titanium dioxide composites prepared by dielectrophoretic assembly of filler particles, *Smart Mater. Struct.*, 2010, **19**(3), 035019.

73 D. N. McCarthy, S. Risse, P. Katekomol and G. Kofod, The effect of dispersion on the increased relative permittivity of TiO_2/SEBS composites, *J. Phys. D: Appl. Phys.*, 2009, **42**(14), 145406.

74 V. Tomer, C. A. Randall, G. Polizos, J. Kostelnick and E. Manias, High- and low-field dielectric characteristics of dielectrophoretically aligned ceramic/polymer nanocomposites, *J. Appl. Phys.*, 2008, **103**(3), 034115.

75 X. Huang, L. Xie, Z. Hu and P. Jiang, Influence of $BaTiO_3$ nanoparticles on dielectric, thermophysical and mechanical properties of ethylene-vinyl acetate elastomer/$BaTiO_3$ microcomposites, *IEEE Trans. Dielectr. Electr. Insul.*, 2011, **18**(2), 375–383.

76 S. Kemaloglu, G. Ozkoc and A. Aytac, Properties of thermally conductive micro and nano size boron nitride reinforced silicon rubber composites, *Thermochim. Acta*, 2010, **499**(1–2), 40–47.

77 J. P. Szabo, J. A. Hiltz, C. G. Cameron, R. S. Underhill, J. Massey and B. White, *et al.*, Elastomeric composites with high dielectric constant for use in Maxwell stress actuators, *Smart Struct Mater 2003 Electroact Polym Actuators Devices*, 2003, **5051**, 180.

78 G. Gallone, F. Carpi, D. De Rossi, G. Levita and A. Marchetti, Dielectric constant enhancement in a silicone elastomer filled with lead magnesium niobate-lead titanate, *Mater. Sci. Eng., C*, 2007, **27**(1), 110–116.

79 N. Gharavi, M. Razzaghi Kashani and A. Moradi, Electromechanical properties of silicone-PZT (lead-zirconate-titanate) composite, *Electroact Polym Actuators Devices*, 2010, **7642**, 764233.

80 H. C. Nguyen, V. T. Doan, J. Park, J. C. Koo, Y. Lee and J. D. Nam, *et al.*, The effects of additives on the actuating performances of a dielectric elastomer actuator, *Smart Mater. Struct.*, 2009, **18**(1), 015006.

81 S. Risse, B. Kussmaul, H. Krüger and G. Kofod, A versatile method for enhancement of electromechanical sensitivity of silicone elastomers, *RSC Adv.*, 2012, **2**(24), 9029–9035.

82 B. Kussmaul, S. Risse, G. Kofod, R. Waché, M. Wegener and D. N. McCarthy, *et al.*, Enhancement of dielectric permittivity and electromechanical response in silicone elastomers: Molecular grafting of organic dipoles to the macromolecular network, *Adv. Funct. Mater.*, 2011, **21**(23), 4589–4594.

83 X. Zhang, C. Löwe, M. Wissler, B. Jähne and G. Kovacs, Dielectric elastomers in actuator technology, *Adv. Eng. Mater.*, 2005, **7**(5), 361–367.

84 X. Niu, H. Stoyanov, W. Hu, R. Leo, P. Brochu and Q. Pei, Synthesizing a new dielectric elastomer exhibiting large actuation strain and suppressed electromechanical instability without prestretching, *J. Polym. Sci., Part B: Polym. Phys.*, 2013, **51**(3), 197–206.

85 B. Kussmaul, S. Risse, M. Wegener, G. Kofod, H. Krüger and D. E. A. Novel, materials by chemical grafting of silicone networks on molecular level, *Electroact Polym Actuators Devices*, 2012, **8340**, 83400Y.

86 F. B. Madsen, A. E. Daugaard, S. Hvilsted, M. Y. Benslimane and A. L. Skov, Dipolar cross-linkers for PDMS networks with enhanced dielectric permittivity and low dielectric loss, *Smart Mater. Struct.*, 2013, **22**(10), 104002.

87 S. J. Dünki, Y. S. Ko, F. A. Nüesch and D. M. Opris, Self-repairable, high permittivity dielectric elastomers with large actuation strains at low electric fields, *Adv. Funct. Mater.*, 2015, **25**(16), 2467–2475.

88 A. H. A. Razak and A. L. Skov, Silicone elastomers with covalently incorporated aromatic voltage stabilisers, *RSC Adv.*, 2017, **7**(1), 468–477.

89 C. B. Gale, M. A. Brook and A. L. Skov, Compatibilization of porphyrins for use as high permittivity fillers in low voltage actuating silicone dielectric elastomers, *RSC Adv.*, 2020, **10**(31), 18477–18486.

90 M. Dascalu, M. Iacob, C. Tugui, A. Bele, G. T. Stiubianu and C. Racles, *et al.*, Octakis(phenyl)-T8-silsesquioxane-filled silicone elastomers with enhanced electromechanical capability, *J. Appl. Polym. Sci.*, 2021, **138**(14), 1–10.

